

Masters Program in **Geospatial Technologies**



DETECTING AND EVALUATING LAND COVER CHANGE IN THE EASTERN HALF OF EAST TIMOR (1972 – 2011)

Helder Antonio Bento Da Costa

Dissertation submitted in partial fulfilment of the requirements
for the Degree of *Master of Science in Geospatial Technologies*

Detecting and Evaluating Land Cover Change in the eastern half of East Timor (1972 – 2011)

Dissertation supervised by

Prof. Dr. Mário Caetano (New University of Lisbon, Portugal)

Dissertation co-supervised by

Prof. Dr. Filiberto Pla (University Jaume I Castellon, Spain)

Prof. Dr. Edzer Pebesma (University of Münster, Germany)

February 2013

ACKNOWLEDGEMENT

I am grateful to the European Union and Erasmus Mundus Consortium (Universidade Nova de Lisboa, Portugal , University of Münster, Germany and Universitat Jaume I, Spain) for awarding me the scholarship to undertake this course. It is a great opportunity for my lifetime experiences. I would like to sincerely thank my supervisor Prof. Mário Caetano whose hard work, guidance, advice and motivation helped realized my goal in this study. I would also like to thank my co-supervisors Prof. Dr. Edzer Pebesma and Prof. Dr. Filiberto Pla for finding time between their schedule to serve on my committee and for their support. This work is not possible without the help from Prof. Dr. Marco Painho who continued to be a constant guidance during the last few months.

I would also like to acknowledge the support I received from my fellow classmates from whom I learn a great deal. Thank you for sharing your knowledge with me in the past eighteen months. A special heartfelt gratitude to Wendy Miles for her constant support throughout my study. You have always been an inspiration to me. My love and gratitude to my family for their never-ending support and encouragement during my stay away from home. Finally, I would like to dedicate this hard work to my late and dearest aunt Teresa.

DETECTING AND EVALUATING LAND COVER CHANGE IN THE EASTERN HALF OF EAST TIMOR (1972 – 2011)

ABSTRACT

Land use / land cover (LULC) change detection based on remote sensing (RS) data is an important source of information for various decision support systems. In East Timor where forest plays a key role in sustaining communities' livelihoods the information derived from LULC change detection is invaluable to the conservation, sustainable development and management of forest resources.

To assess the patterns of land cover change, as a result of complex socio-economic factors, satellite imagery and image processing techniques can be useful. This study is concerned with identifying change in land use and land cover types in East Timor between 1972 and 2011, using satellite images from Landsat MSS, TM and ETM+ sensors. Seven major cover types were identified in this study including forest, mixed rangeland, grassland, farmland, built-up areas, bare soil and water. A combination of NDVI differencing, supervised and unsupervised classification was used to derive final classification maps. Due to the lack of ground truth data, further processing were performed to improve the final classification maps by applying rationality change test.

Post-classification comparison change detection technique was used to assess categorical changes between 1972 and 2011. The results highlight a significant level of deforestation due to uncontrolled illegal logging and increase in farmland, built-up areas, as well as bare soil. This decline has had considerable impact on the livelihoods of rural communities. As the new nation of Timor-Leste establishes itself, it must consider its current stock and distribution of natural resources to ensure that development efforts are geared towards sustainable outcomes. Without this information historical patterns of resource consumption, development efforts may, unwittingly, lead to continuing decline in forest resources.

KEY WORDS

Change Detection

Change Rationality Test

Landsat

Land Use/Land Cover

NDVI Differencing

ACRONYMS

DN	Digital Number
DOS	Dark Object Subtraction
ETM+	Enhanced Thematic Mapper Plus
FAO	Food and Agricultural Organization
FCC	False Color Composite
GLOVIS	Global Visualization Viewer
LULCL	Land Use/Land Cover
MAF	Ministry of Agriculture and Fisheries
MLC	Maximum Likelihood Classification
MSS	Multispectral Scanner
NDVI	Normalized Difference Vegetation Index
NIR	Near Infrared
TCC	True Color Composite
TM	Thematic Mapper
TOA	Top-of-Atmosphere
UTM	Universal Transverse Mercator
WGS 84	World Geodetic System 84

TABLE OF CONTENTS

ACKNOWLEDGEMENT	iii
ABSTRACT	iv
KEY WORDS	v
ACRONYMS.....	vi
TABLE OF CONTENTS.....	vii
LIST OF TABLES	ix
LIST OF FIGURES	x
CHAPTER 1	1
INTRODUCTION	1
1.1. Background.....	1
1.2. Statement of the Problem and Justification.....	3
1.3. Objective of the Study.....	5
CHAPTER 2.....	7
STUDY AREA AND DATASET	7
2.1. Study area.....	7
2.2. Dataset	8
CHAPTER 3.....	11
LITERATURE REVIEW	11
3.1. Remote sensing application.....	11
3.2. Change detection techniques	12
3.2.1. Pre-classification change detection technique	12
3.2.2. Post-classification comparison	14
3.3. Accuracy assessment.....	15
CHAPTER 4.....	17
METHODOLOGY	17
4.1. Image Pre-processing.....	18
4.1.1. Cloud Masking.....	21
4.1.2. Conversion to at-sensor radiance ($Q_{cal} - \rho\lambda$).....	21

4.1.3.	Conversion to at-sensor Radiance ($L\lambda - \rho\lambda$)	23
4.1.4.	Atmospheric correction by Dark-Object Subtraction (DOS)	24
4.1.5.	Classification scheme	26
4.2.	Image Processing.....	27
4.2.1.	Normalized Difference Vegetation Index (NDVI)	28
4.2.2.	Image Classification	30
4.2.3.	Change rationality test	33
4.3.	Post-classification change detection	35
CHAPTER 5.....		36
RESULTS AND DISCUSSION		36
5.1.	NDVI.....	36
5.2.	NDVI Differencing	36
5.3.	Selection of coefficients	38
5.4.	Image classification	40
5.4.1.	Change rationality test: Rule I	40
5.4.2.	Change rationality test: Rule II.....	42
5.4.3.	Change rationality test: Rule III and Rule IV	42
5.5.	Post-classification comparison.....	43
5.6.	Post-classification change detection	45
5.7.	Influence of 2000 map.....	52
5.8.	Change rationality rules	52
5.9.	Potential of Approach.....	53
CHAPTER 6.....		54
6.1. CONCLUSION.....		54
6.2.	Limitations	54
BIBLIOGRAPHICAL REFERENCES		57
APPENDIX A.....		61
APPENDIX B.....		64
APPENDIX C		68
APPENDIX D.....		69

LIST OF TABLES

Table 2.2.1. Raw Landsat data used in this study.....	9
Table 2.2.2. Reference data	10
Table 5.2.1. Thresholds of index decrease and increase for all NDVI differencing images.....	37
Table 5.3.1. One time accuracy assessment for 2000 image.....	41
Table 5.4.1.1. Total number of unchanged pixels for each category as defined by Rule I	42
Table 5.4.3. Summary of change rationality test.....	43
Table 5.5.1. Summary of final classification map area statistics for six observation dates.....	44
Table 5.5.2. The percentage of land use categories for each observation date.....	45
Table 5.6.1. Matrix of land cover change from 1972 to 1987.....	46
Table 5.6.2. Matrix of land cover change from 1987 to 1996.....	47
Table 5.6.3. Matrix of land cover change from 1996 to 2000.....	48
Table 5.6.4. Matrix of land cover change from 2000 to 2005.....	48
Table 5.6.5. Matrix of land cover change from 2005 to 2011.....	49

LIST OF FIGURES

Figure 1.2. Vegetation distribution in western part of East Timor in 1989.....	4
Figure 1.2. Vegetation distribution in western part of East Timor in 1999.....	4
Figure 2.1. Map of the study area.....	8
Figure 4. The main workflow of the methodology.....	17
Figure 4.1.1. Landsat ETM+ 2011 band 5 with before gap filling.....	19
Figure 4.1.2. Landsat ETM+ 2010 band 5 used for filling the gaps in 2011 image ...	20
Figure 4.1.3. The result of gap-filling procedure for 2011 image band 5	20
Figure 4.2. The rescaling factors contained in the product metadata of Landsat TM5 acquired on October 11, 2005.	23
Figure 4.2.1. Probability density function of NDVI differencing image.....	30
Figure 4.2.1.1. Range of optimal c value.....	31
Figure 4.2.2. Derivation of final classification maps for five acquisition dates (1972, 1987, 1996, 2005 and 2005) by combining change/no change maps and classified maps from supervised and unsupervised methods.....	33
Figure 5.1.1. NDVI maps for all observation dates.....	38
Figure 5.3.1. NDVI index decrease part shows large amount of noises due the selection of high c value (smaller negative). The blue circle shows and airport run.....	39
Figure 5.3.2. NDVI index decrease part shows minimum noise due to selection of low c value (larger negative).	40
Figure 5.3.3. NDVI index decrease part using medium c value. Notice the reduction in the noise but enough change information are retained.	40

Figure 5.4.1.1. Unchanged LULC categories between 1972 and 2011 as identified by change rationality test.....	42
Figure 5.5.1. Distribution of land cover types in East Timor between 1972 and 2011.....	45
Figure 5.6.1. Gain and loss of LULC change classes between 1972 and 2011.....	50
Figure 5.6.2. “From-to” major categorical change map between 1972 and 2011....	50
Figure 5.6.3. “From-to” change between 1972 and 2011 in Lautem district.....	51
Figure 5.6.4. “From-to” change between 1972 and 2011 in Baucau and Viqueque districts.....	52

CHAPTER 1

INTRODUCTION

1.1. Background

Research focus on land use and land cover (LULC) change gained prominence after the realization that land cover change affects climate (Lambin et al., 2003). Since then, many studies have been conducted around the world to understand the causes, impacts and rates of land cover change. It is an important variable in studying the dynamic changes that are continuously occurring on the earth's surface. In addition, it has become a major issue in many of the current strategies for managing natural resources and monitoring environmental damages. The development of the concept of LULC has greatly increased research on land use and land cover change, thus providing an accurate evaluation of the spread and health of the world's forests, grasslands, and agricultural resources.

Worldwide deforestation is still alarmingly high (FAO, 2010). A recent study by Goldewijk and Ramankutty (2004), where they assessed historical land cover data, showed that forest has decreased from 50-62 million km² in 1700 to 43-53 million km² in 1990. This reduction is due to the expansion in land used for crops and ranching (Goldewijk and Ramankutty, 2004). Many of these phenomena occur in developing countries where agricultural expansion has caused reduction in forest cover over long periods of time. In Brazil, for instance, the European exploitation of forest for rubber plantation followed by sugar cane production caused the reduction in Araucaria forest from 25 million ha to only 445000 ha. The introduction of new cash crops to Brazil in 19th century contributed to the conversion of millions of hectares of forest into coffee plantation, adding more pressure to the remaining forest. The consequences of this deforestation have

included increased erosion problems on hill slope and disturbance to drainage systems (Goldewijk and Ramankutty, 2004).

The examples above are just some of the many cases of causes and impacts of land use/land cover changes. Obviously, deforestation in smaller countries may not be heard of. However, the impacts are the same in the way that they affect communities. Often times, the LULC change in an area is an outcome of complex socio-economic condition in which human activities play a central role. Forest as a resource is becoming scarce because of the immense agricultural expansion and demographic pressure. Understanding this dynamic requires a tremendous amount of resources in terms of time, finances, and the right technology, not only because the problems are complex but also because it is geographically extensive in nature.

Thus, satellite images and aerial photography offer the most cost effective method for land cover mapping and change detection throughout the world, both for bi-temporal and multi-temporal analysis (Ioannis and Meliadis., 2011). Over the years, remote sensing in the form of aerial photography has been an important source of LULC information. Ioannis and Meliadis (2011) state that this approach provides several advantages: (1) the synoptic view of large geographic areas, (2) the digital form of the data facilitating more efficient analysis and (3) land cover maps can be generated at considerably less cost than by other methods. The cost of aerial photography acquisition and the interpretation of cover types is prohibitively expensive for extensive geographic areas, thus, a common alternative is to acquire the needed information from freely available digital satellite imagery such as Landsat TM and ETM+.

Hence, Remote Sensing (RS) and Geographic Information System (GIS) are now providing new tools for better LULC studies. The collection of remotely sensed data facilitates the synoptic analysis of Earth's surface and its change at local, regional and global scales over time.

1.2. Statement of the Problem and Justification

Like many other poor and developing countries around the world, forests play a major role in sustaining agricultural-based communities' livelihoods in East Timor. The majority of people in East Timor practices shifting cultivation, by clearing and burning of lands and cutting of forests and bushes. Coupled with wildfires and excessive logging activity, this has caused a serious environmental problem (Sandlund et al, 2001; Bouma and Kobryn, 2004). These traditional agricultural practices have been around since at least 19th century and studies have indicated its intensification in recent years (Jeus et al., 2012). Yet, there has not been many studies to understand the impact of such a practice on forest and so public awareness of its impact is very low. This clearly poses serious challenges for the task of efficient planning and management of the environment, which is often constrained by insufficient information on the rates of land cover/use change.

As a relatively new nation, East Timor is facing great challenges and developmental issues in many areas. One of the key areas concerns the dynamic of land use and changing land cover situation which has not been given enough attention since the country's independence in 2002. Previous studies on land use/cover change in East Timor have only looked at the phenomena between two different dates (i.e. bi-temporal analysis). For instance, Bouma and Kobryn (2004) compared two classified Landsat images (1989 and 1999) of the western part of East Timor and found that the major vegetation cover types such as forest and woodland have declined in nine districts (Figure 1 and 2). Mapping projects, conducted through collaboration between public institutions and non-governmental agencies, have also produced some spatial data, but only for recent years. Although, findings from these studies have identified the common causes of environmental damages, and have initiated the development of some key environmental policies, they are still far from strengthening the public's understanding of land cover dynamics.

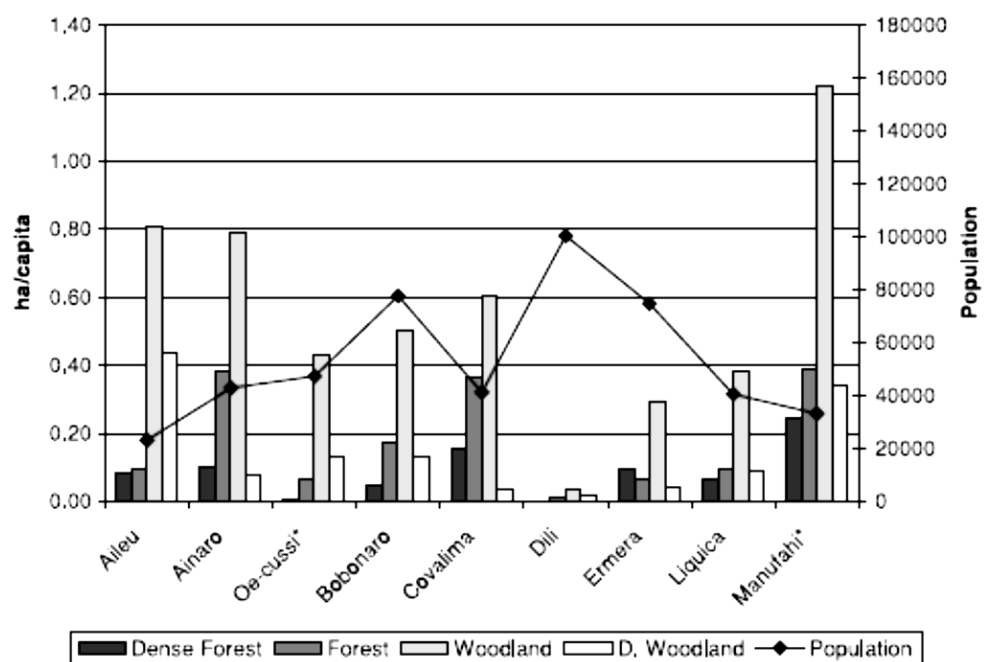


Figure 1.1. Vegetation distribution in western part of East Timor in 1989. *Source: Bouma and Kobryn (2004).*

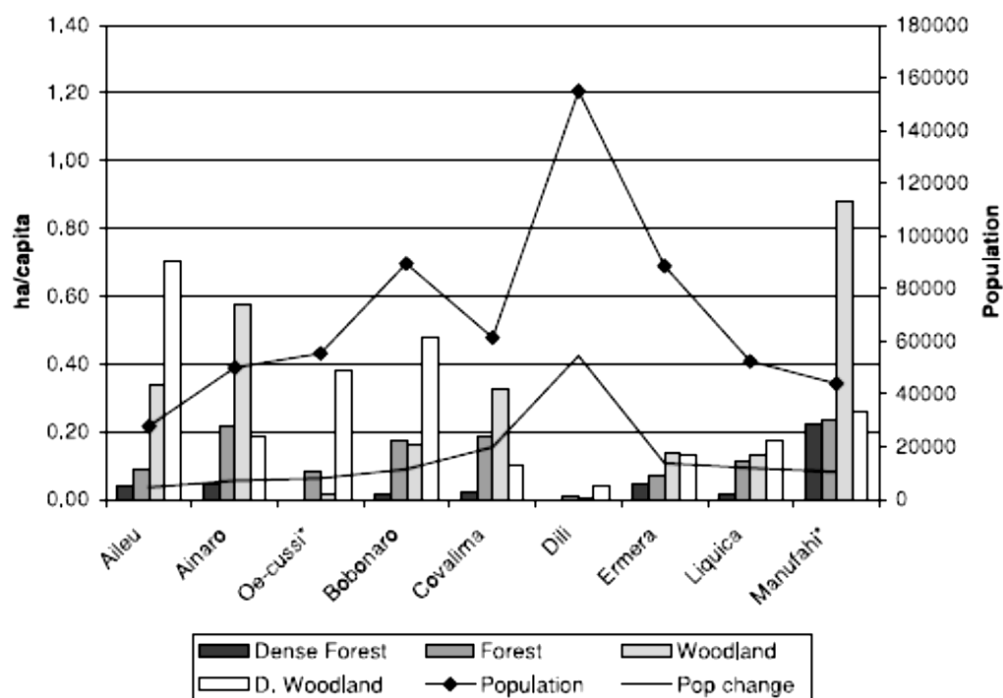


Figure 1.2. Vegetation distribution in western part of East Timor in 1999. *Source: Bouma and Kobryn (2004).*

The limited availability of historical data (e.g., land use maps, topographic maps, aerial photos) in East Timor, the high cost of good quality data collection and information dissemination, as well as the limited number of trained personnel in remote sensing constrain East Timor's ability to conduct LULC change detection studies, or environmental studies in general. This challenge needs to be addressed and overcome with viable solution.

A multi-temporal analysis of land cover change is deemed valuable in this regards. By studying land use/cover change through multiple time stamps, a generalized understanding of causes of land use/cover change over a longer trajectory can be obtained. Freely available satellite data such as Landsat images can make it possible to carry out this kind of study and the result from such a study can add to the public's knowledge the importance of spatial data and information for policy making

1.3. Objective of the Study

The aim of this study is to analyze and detect land cover change using multi-temporal Landsat images covering the eastern half of East Timor from 1972 to 2011. Specifically, the following questions will be used as guide in the study:

- What are the extent and nature of vegetation distribution in the eastern half of East Timor?
- How is the vegetation trend changing during the study period in respect to other cover types?
- Can land cover and land use change be mapped with limited reference data?
- Is there an alternative to assess the accuracy of change detection derived from limited reference data?

Furthermore, specific tasks will be performed to help answer the above questions.

- Calculate Normalized Difference Vegetation Index (NDVI) for all the observation dates (1972, 1987, 1996, 2000, 2005 and 2011)

- Map land use and land cover types in the study region using commonly used algorithm such as supervised classification and/or unsupervised classification techniques
- Perform and combine NDVI differencing techniques with LULC map to improve image classification result
- Improve the final classification using change rationality test
- Perform change detection between all the different dates
- Evaluation of change detection result

CHAPTER 2

STUDY AREA AND DATASET

2.1. Study area

The study area is located in the eastern part of East Timor extending between E126°, S8.3° and E127.5°, S9.1°. It covers three districts, Baucau, Viqueque and Lautem (Figure 2.1). The topography of the region is highly varied characterized by hilly terrain and coastal plains. The highest point in the region, which is also the second highest point in East Timor, is mount Matebian (2335m). The rainfall distribution in the study area also varies. In Baucau, precipitation is well distributed in the hilly areas but less so near the coast. In Viqueque district rainfall is well distributed throughout the area. Sometimes the rainy season (wet season) in this area is longer than its dry period. According to the 1970 census by Portuguese government the population in the study area was 177688, approximately 29.3% of the total East Timor's population (Costa Carvalho, 1970). The current population is estimated at 241517 people of which 83% live in rural areas (NSD, 2011).

Agricultural land use in this region is predominant with Baucau and Viqueque among the four districts in East Timor that produce 75% of the country's rice (Pederson and Arnerbeg, 1999). Another local product includes maize which is grown in tilled fields or with little cultivation under traditional slash and burn systems (Da Costa, 2003). Toward the eastern part of the study area is Lautem, the district with much less agricultural intensification. In the past, however Lautem had been an important livestock and fish producing area. A large portion of forested land in the study area is located in Lautem where the first National Park was established. This area is also home to 3 out of the 15 identified "important bird species" in East Timor (Mau, n.d.). Little is known about whether or not deforestation has threatened the natural habitat of these species.

Apart from the existence of deforestation in the area and the author's familiarity of the area, one of the reasons for selecting this study area is because a similar study was already conducted on the western part of East Timor by Bouma and Kobryn (2004) from which these three districts were excluded. Therefore, this study can be used to enrich information regarding land use/cover change for the entire country of East Timor.

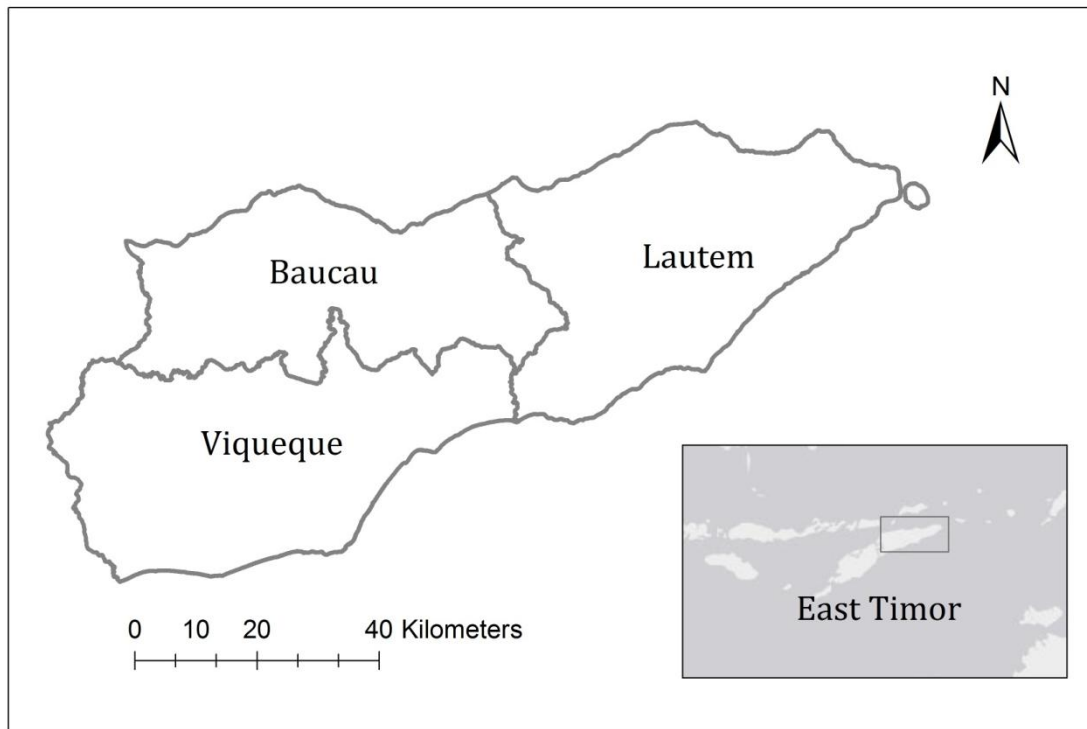


Figure 2.1. Map of the study area

2.2. Dataset

This study spans a four decade time period—1970s, 1980s, 1990s, and 2000s. For the 1970s two Landsat MSS images from October 4 and October 23, 1972 were obtained to cover the entire study area. For the 1980s a Landsat TM image from September 8, 1987 was obtained. For the 1990s, a Landsat TM image from August 15, 1996 was obtained. For the 2000s, the ETM+ image was obtained for the year 2000 and 2011, while for the year 2005, the Landsat TM image was used (Table 2.2.1 and 2.2.2). Ideally, data should be obtained from a satellite that acquires data

at the same time of day, being that all of the data is from Landsat that is not an issue. Images with corresponding anniversary dates, which are dates over time which correspond with season, month, and preferably weeks should be obtained because it helps minimize discrepancies in reflectance caused by seasonal vegetation fluxes and sun angle. However, often times anniversary dates are impossible to obtain because of the times that the sensor system passes over a particular area so the logical alternative is to find images of the area in the same or near to the same month or season (Jensen 2007) In addition, atmospheric conditions can also affect a sensor's visibility as clouds tend to be persistent over a tropical island such as East Timor. These issues were taken into consideration and formed the basis for deciding the dataset for this study. All data was obtained from the USGS Global Visualization Viewer (GLOVIS). Table 1 and 2 shows the description of the data.

The reference data utilized in this study is a topographic map of East Timor with the scale of 1:5000 and the 2000 land use map of East Timor. Both maps contain information of land cover types for the year 2000. The land use map was produced by the Ministry of Agriculture and Fisheries (MAF) using spot images with ground truth data.

Year	Date of acquisition	Sensor	Path	Row
1972	1972-Oct-23	Landsat MSS	117	66
	1972-Oct-4	Landsat MSS	166	66
1987	1987-Sept-8	Landsat TM	109	66
1996	1996-Aug-18	Landsat TM	109	66
2000	2000-Sept-3	Landsat ETM+	109	66
2005	2005-Oct-11	Landsat TM	109	66
2010*	2010-Aug-14	Landsat EMT+	109	66
2011	2011-Aug-17	Landsat ETM+	109	66

Table 2.2.1. Raw Landsat data used in this study

* *used for gap filling the 2011 image*

Reference data	Date of production	Source	Scale
Land use map of East Timor	2000	ALGIS, Ministry of Agriculture and Fisheries (MAF)	NA
Topographic map	2001	Ministry of Justice of East Timor	1:50000

Table 2.2.2. Reference data

Tools

ArcGIS 10

PANCROMA

CHAPTER 3

LITERATURE REVIEW

3.1. Remote sensing application

Since the advent of the remote sensing satellite (Landsat 1) in 1972, many land cover and land use change studies started being conducted at varying levels. For instance, at local level, studies were conducted in various domains including landscape, agriculture, watershed management, forestry, and using data from various sensors such as Landsat, MODIS and AVHRR. Masek et al (2000) used Landsat images acquired between 1973 and 1996 to study land use efficiency in the metropolitan area of Washington DC, USA. By applying NDVI differencing and visual inspection of true urban growth, their study revealed that the Washington metropolitan area has expanded at a rate of 8.5 square miles every year.

Doraiswamy et al, (2003) evaluated the integration of Landsat TM data into a crop growth model to simulate wheat yields in the semi-arid region of North Dakota, USA. Their study found similar result as the one reported by the county. Rahman et al (2004) used Landsat (MSS, TM and ETM+) images to detect changes in winter crops in Durgapur Upazilla, Bangladesh. Using the Maximum Likelihood Classifier (MLC), they found an increasing trend in winter crops 1977 and 2000 which is attributed to the increase in irrigation during winter season as well as population pressure in the area. Petit et al (2001) also used MLC for a change detection study in south-eastern Zambia, and reported an annual rate of 4.0% land cover change. Another study was conducted by Anderson et al (2012) using moderate resolution satellite imageries for the purpose of water resource management. Their study concluded that Landsat thermal imagery can improve our ability to monitor changes in water used due to changing climate and population growth.

At regional level, application of remote sensing has also engaged in a wide range of domains including deforestation, desertification and climate change among many other things. For instance, Symeonakis and Drake (2004) developed a system for monitoring desertification using four indicators (rainfall, vegetation cover, surface run-off and soil erosion) that were derived from continental-scale remotely sensed data. By combining these indicators, they were able to identify areas under threat of desertification. Another example of regional level application of remote sensing study was the study on impacts of global warming in Arab region where MODIS images were used (Ghoneim, 2009). CORINE Land Cover Mapping is also among the many projects that entail regional collaboration to produce land cover maps based on the interpretation of satellite images (EEA, 2013).

3.2. Change detection techniques

Over the years, a number of change detection techniques have been developed and widely used for monitoring land use/land cover changes. Numerous researchers have discussed the strength and weaknesses of each of this technique (Singh, 1989; Nelson, 1983; Lu et al, 2004). These techniques can be broadly divided into two main categories: pre-classification spectral change detection and post-classification comparison techniques (Nelson, 1983; Singh, 1989, Coppin and Bauer, 1996). Previous studies have successfully employed many of these techniques in analyzing land cover change. Some of these studies have also focused on comparing the ability of various techniques to accurately identify areas of change.

3.2.1. Pre-classification change detection technique

The pre-classification change detection technique is also referred to as enhancement change detection. Generally, the pre-classification change detection has the ability to accurately identify areas of spectral changes (Singh, 1989). However, this technique requires additional analysis to determine the nature of the spectral changes and it also requires more accurate image normalization and co-

registration. One of the most widely used change detection algorithm is image differencing. It is a technique by which images captured at different times, which are co-registered, are subtracted from one another to obtain unchanged areas. Basically, it subtracts the Digital Number (DN) values of one band in the first image from the corresponding DN value of the same band in the second image. The subtraction results in positive and negative values for areas that change between the two images and zero value for areas that do not change (Sohl, 1999). A critical element of using this technique is how to decide where to place the threshold for change in the differenced image (Singh, 1989). Additionally, it is also important to apply radiometric normalization to the images before conducting image differencing. Simplicity and straightforwardness are the strength of this technique (Lu et al, 2004). However, it is quite sensitive to misregistration and mixed pixels and it also lacks the information on the type of change that is occurring (Sohl, 1999; Lu et al, 2004).

MacLeod and Congalton (1998) performed a quantitative comparison of change detection algorithms and reported that image differencing performed better in detecting changes in submerged aquatic vegetation, with an overall accuracy of 78%. However, Sohl (1999) and Veetil (2012) showed that the image differencing technique was straightforward but on the expense of detailed information, and its implementation can get more complicated when applied to multiple bands, due to the difficulty of interpreting the colors of multi band false color composite. Hence, Sohl (1999) states the simplicity of image differencing is also its main weaknesses because it does not provide adequate explanation on the nature of the change.

Similar to image differencing is the vegetation index differencing. This technique uses a data transformation shown to be related to green biomass where, for two different dates, a Normalized Difference Vegetation Index (NDVI) image is calculated and subtracted from one another to produce image showing areas of

change and no-change (Mas, 1999). The NDVI is calculated by $NDVI = (NIR - RED)/(NIR + RED)$, where NIR represents near-infra red band response for a given pixel of and RED represents red band (Mass, 1999). This method is also widely used in land cover change studies (Pu et al, 2008; Masek et al, 2000).

3.2.2. Post-classification comparison

The post classification technique involves a comparative analysis of spectral classification of two independently classified maps (Mas, 1999). This technique has the advantage of providing direct information on the nature of land cover changes and it can be used with both supervised and unsupervised classifications. The main advantages of these techniques are that it minimizes atmospheric influences on the images, and also the sensor and environmental differences between multi-temporal images (Lu et al, 2004). This technique is capable of producing descriptive information on the type of changes that are occurring, and it does not necessarily require co-registration and radiometric normalization of input images. Lu et al (2005) states that the disadvantages of this technique are that it requires great amount of time and skills to produce classification, and that the accuracy of the change detection depends on the accuracy of the classified maps because any errors made in the classification are compounded into the change detection.

Numerous studies have produced good results with post-classification comparison technique. Sohl (1999) reported accuracies of 96% for the identification of new forest land and 62% for new agricultural land using a post classification technique in a semi-arid environment. Guo et al (2010) also used post-classification comparison by which they obtained an accuracy of 89% in their study of land cover change to detect bushfire. Mersten and Lambin (2000) found a net reduction in forest cover between 1973 and 1996 in Cameroon using post-classification comparison technique. Furthermore, Sohl (1999) also noted the advantage of post-classification technique to provide analysts with detailed descriptive comparison

between images. A comparative study of change detection techniques by Mas (1999) also showed a high accuracy by post-classification comparison technique which was attributed to the high accuracy of the classification of each individual image.

While large number of studies has produced positive results with this technique, MacLeod and Congalton (1998) reported that the post classification comparison technique produced rather poor results compared to NDVI differencing, and they stated that this poor accuracy could be attributed to the errors from both classifications. In the review of change detection techniques Singh (1989) cited Toll et al (1980) by stating that the poor performance of post-classification comparison technique is partly due to the difficulty of producing image classifications that are comparable to one another. With that said, there is no single image classifier or change detection technique that fits every situation. Often times, researchers perform comparison analysis of their performances and then decide to use the classifier or technique that produces the best result.

3.3. Accuracy assessment

Accuracy assessment, then, is an important step in image classification and change detection (Congalton and Green, 2008). A classified image or change detection map needs to be compared against reference data, assumed to be true, in order to assess its performance and quantify its accuracy. One of the common procedures in describing the accuracy of a classified map is by using a confusion matrix where a set of categories on a classified map and a reference map are plotted on a matrix from which descriptive measures can be obtained (Congalton and Green, 2008, Lillesand et al, 2004). Generally, a full accuracy assessment needs to include the report on User Accuracy, Producer Accuracy and indices such as Kappa (Congalton and Green, 2008). Pontius and Millones (2011), however, critically argued against the further use of Kappa index in accuracy analysis because it does not have useful

interpretation. Instead, they proposed the use of quantity disagreement and allocation disagreement to obtain useful summary of the accuracy. Either way, accuracy assessment for a successful remote sensing project relies heavily on the reference data (Congalton and Green, 2008).

In multi-temporal studies where data spans over a long period of time, obtaining reference data for multiple observation dates can be difficult. This certainly poses challenges for change detection studies especially in areas where land use/land cover information and reference data are of poor quality or even non-existent. This problem has been discussed by numerous researchers (Liu and Zhou, 2004; Baraldi et al, 2005; Foody, 2010) and while these authors recognize the utmost importance of reference data, they have also shown that change detection can be performed when the reference data are limited. Foody (2010) even concluded that it is possible to estimate the accuracy of change detection without ground data. Liu and Zhou (2004) on the other hand have proposed methodology for evaluating land cover change trajectories where a set of rules can be defined to evaluate the rationality of land cover change. This study will employ a slight modification of the rules proposed by Liu and Zhou (2004).

CHAPTER 4

METHODOLOGY

This section describes the methodology used in this study. First, various works in the preprocessing stage (gap-filling, radiometric and atmospheric correction) are described then followed by explanation of NDVI differencing technique and image classification procedures. Finally, the explanation on change rationality test for improving the final classification maps is presented. Figure 4.1 shows the main workflow of the methodology.

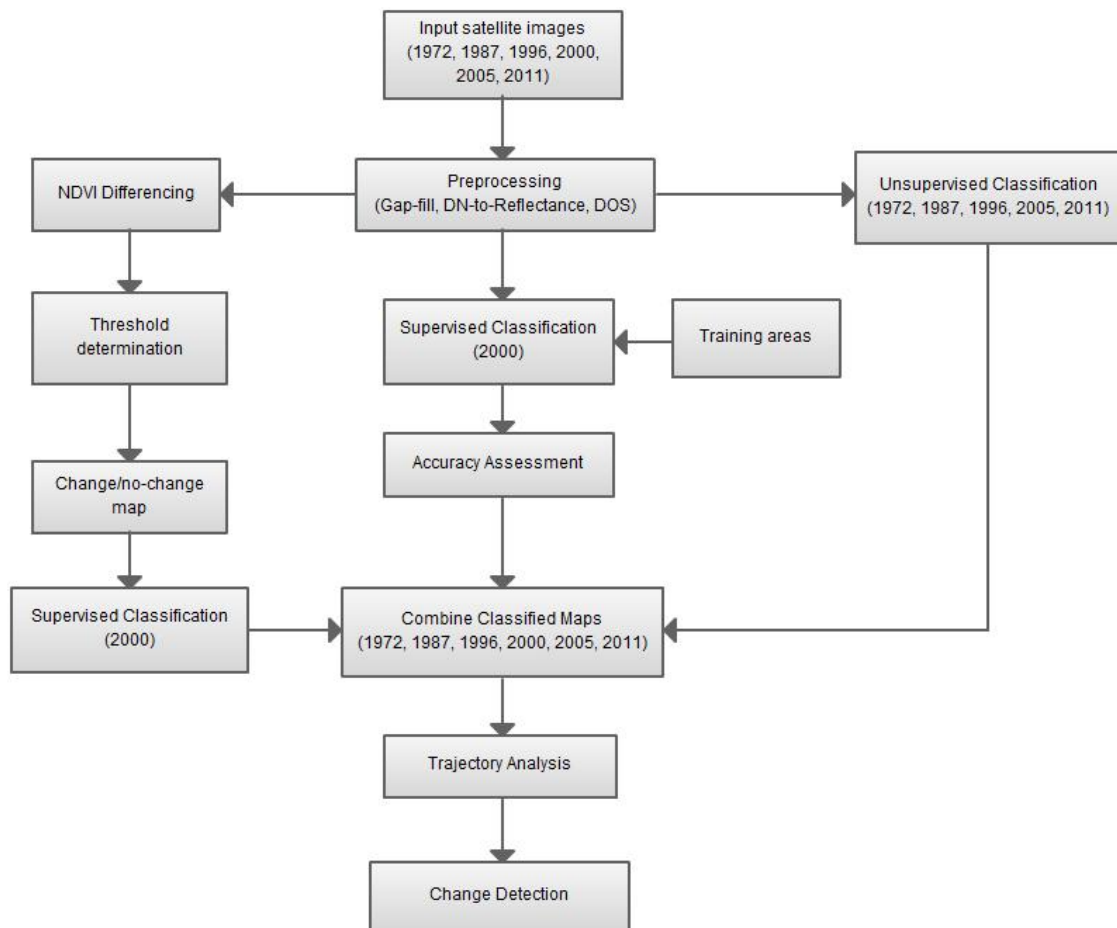


Figure 4. The main workflow of the methodology

4.1. Image Pre-processing

Prior to performing image classification it is important that the raw data are preprocessed and prepared in a proper way so that error due to the geometry of the earth, radiometric and atmospheric effects can be accounted for. The general procedure in the preprocessing stage is to apply geometric, radiometric and atmospheric correction. In this study the geometric correction was not applied to the satellite images because they were already georeferenced to UTM Coordinate System Zone 52S. Similarly, the land use shapefile from ALGIS was also georeferenced. Thus, georeferencing was only performed for the scanned topographic map of the study area, which resulted in a root mean square error (RMSE) of 0.1123.

In addition, prior to radiometric and atmospheric corrections, which is described in the following section, a Gap-filling was performed for Landsat image of 2011. This image of 2011 was captured by Landsat ETM+. Due to its faulty Scan Line Corretor (SLC) since 2003, the Landsat ETM+ sensor has been obtaining images of the earth's surface in the SLC-Off mode (Scan Line Corrector). As a result, the image only has about 87% of their pixels causing gap effects. These gaps created a stripping effect along the edge of the image (Figure 4.1.1). Several procedures have been developed to fill in these gaps including the work by Zhang et al., (2007) and Scaramuzza et al., (2004). In this study the gap in the 2011 image was filled with another Landsat ETM+ image which was acquired on August 14, 2010 (Figure 4.1.2). Each band in the 2011 image was filled with pixel information from its corresponding band in the 2010 image. Although the 2010 image also has gaps, it was possible to gap-fill the first image because the gaps in the images from two different dates are not necessarily in the exact same spot. It is important to note that the ideal procedure would be to use the image from the nearest month (e.g., September or October), however, due to the lack of cloud free image, the 2010 image was used, assuming that between these 2010 and 2011 land cover had been

small enough to still make comparison with other decades using this data (Figure 4.1.3). This process of gap-filling was executed in the PANCROMA software using the Hayes method. The Hayes method is a local optimization method where it uses a sliding window technique, with a defined size, to estimate the value in the gaps using values from other pixels that exist in the sliding windows (PANCROMA, 2012).

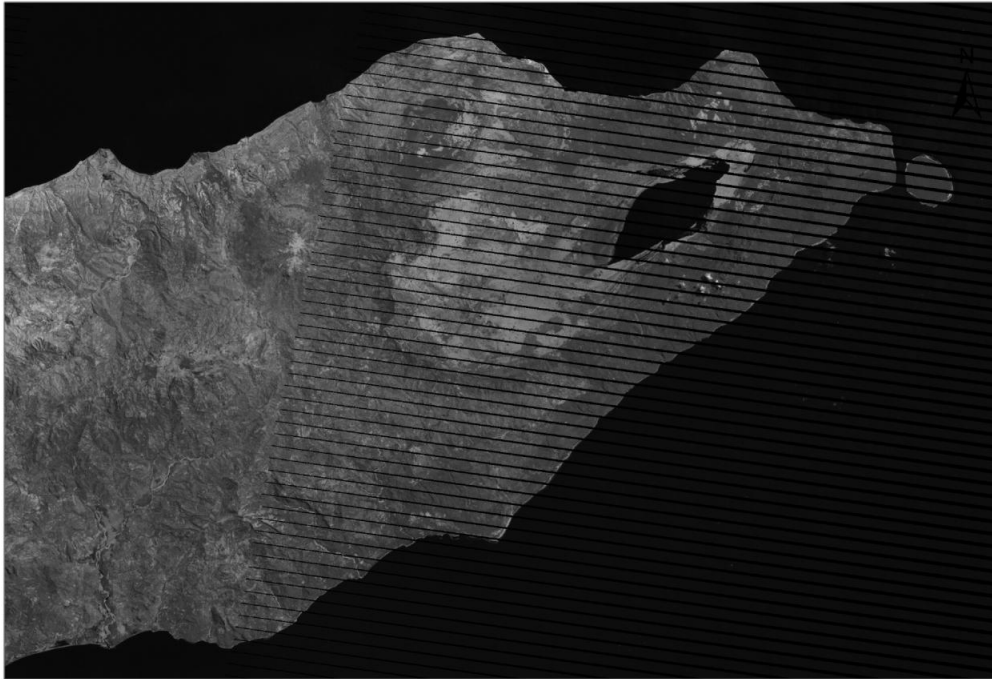


Figure 4.1.1. Landsat ETM+ 2011 band 5 with before gap filling

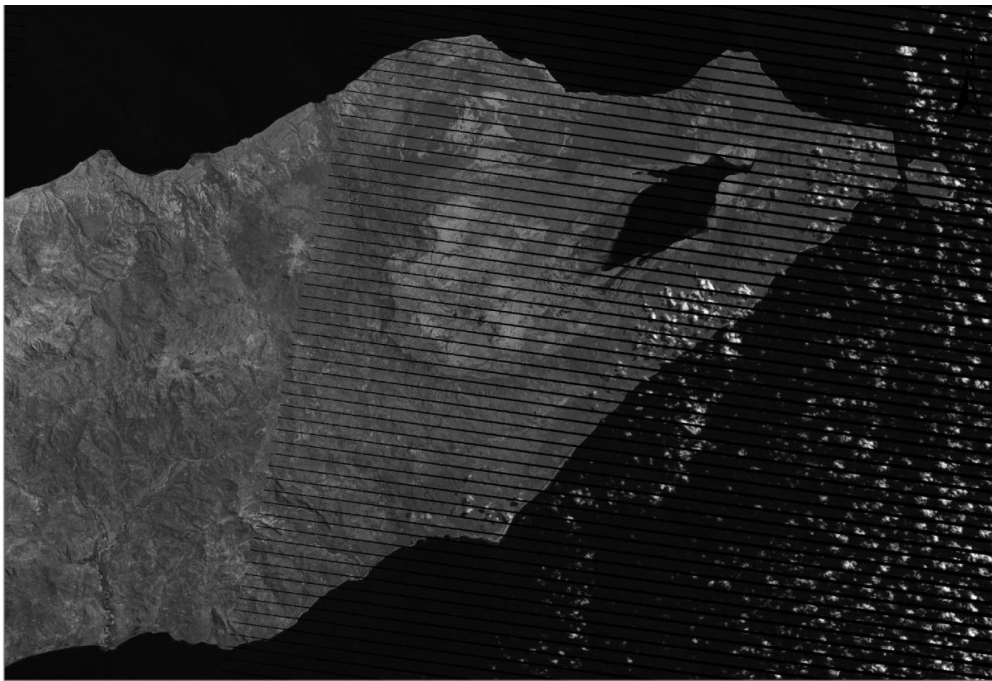


Figure 4.1.2. Landsat ETM+ 2010 band 5 used for filling the gaps in 2011 image

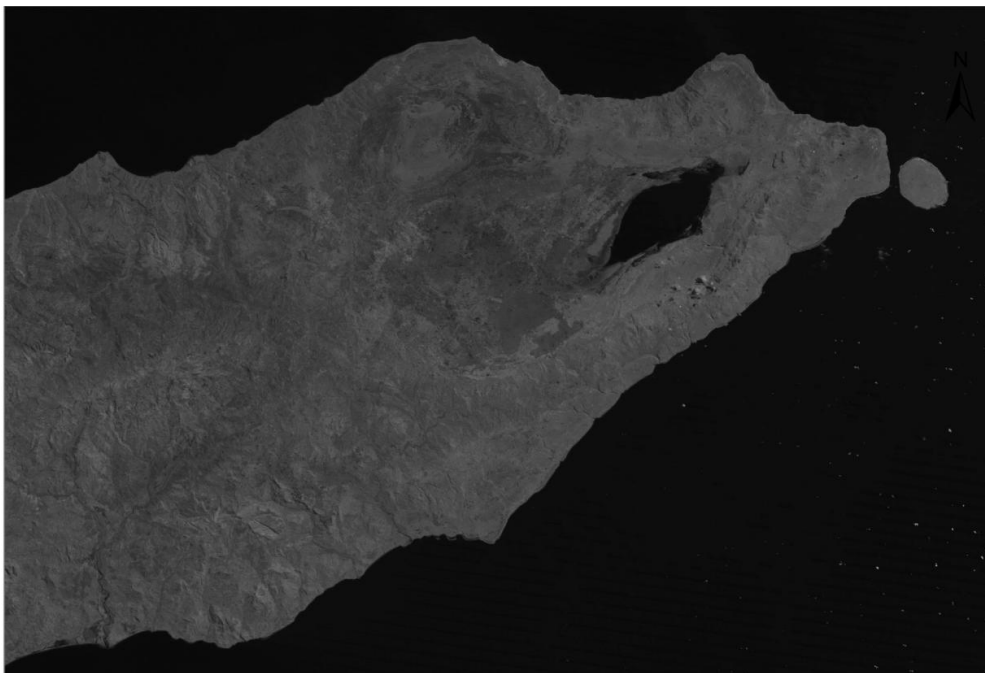


Figure 4.1.3. The result of gap-filling procedure for 2011 image band 5

4.1.1. Cloud Masking

Clouds are a common feature found in all satellite images and they can affect image classification because they may cover large extensive area under study. The easiest way to deal with cloud cover is to include it in the classification as a separate class or by masking the clouds outs. Most Landsat data used in this study have a very minimum cloud cover. Yet, some clouds do exist and they were removed by using techniques proposed by Martinuzzi et al. (2007).

The algorithm uses pixel information from band 1 (blue) and band 6 (thermal) to create the mask. Clouds are very reflective in the blue band and very cold in the thermal band. This method was chosen because it is an efficient and relatively simple algorithm to create cloud mask for Landsat images. A prior visual analysis was performed to identify the DN of clouds ranging from the minimum to 255. In band 1 (blue) clouds are very reflective such that their DN are very high. Thus by identifying pixel values where clouds appear thinner the mask was created where $DN_{min} < DN \text{ of pixel in band 1} < 255$. In the thermal band (6), clouds are colder and appear dark on the image. Hence, the mask was created for pixels where $1 > DN \text{ of pixels in band 1} < DN_{max}$.

By intersecting these two masks, and with an additional buffer of 3 pixels, final cloud masks were obtained for images that have cloud contamination (1996, 2000, 2005). The masks were then used on the final classified maps to exclude pixels from images which did not contain clouds so that they can be compared with images that have clouds.

4.1.2. Conversion to at-sensor radiance ($Q_{cal} - \rho_{\lambda}$)

When working with images data from multiple sensors and platforms it is necessary to convert them into a physically meaningful common radiometric scale (Chander et al., 2009). This is important because different sensors have different

calibration methods to scale, convert and store data. Radiometric calibration of MSS, TM and ETM+ sensors involves rescaling raw digital numbers (Q) transmitted from satellite to calibrated digital numbers (Q_{cal}), which have the same radiometric scaling for all scenes processed on the ground for a specific period. Conversion from Q_{cal} in Level 1 products back to at-sensor spectral radiance (L_λ) requires knowledge of the lower and upper limit of the original rescaling factors. The following equation is used to perform the Q_{cal} -to- L_λ conversion for Level 1 products:

$$L_\lambda = G_{rescale} * Q_{cal} + B_{rescale} \quad (1)$$

where

$$G_{rescale} = (LMAX_\lambda - LMIN_\lambda) / (Q_{calmax} - Q_{calmin}) \quad (2)$$

$$B_{rescale} = LMIN_\lambda - \frac{(LMAX_\lambda - LMIN_\lambda)}{(Q_{calmax} - Q_{calmin})} * Q_{calmin} \quad (3)$$

Therefore equation 1 can be rewritten as:

$$L_\lambda = (((LMAX_\lambda - LMIN_\lambda) / (Q_{calmax} - Q_{calmin})) * (Q_{cal} - Q_{calmin}) + LMIN_\lambda \quad (4)$$

where

L_λ = spectral radiance at the sensor's aperture [$W/m^2 sr \mu m$]

Q_{cal} = quantized calibrated pixel value (DN)

Q_{calmin} = minimum quantized calibrated pixel value corresponding to $LMIN_\lambda$ [DN]

Q_{calmax} = Maximum quantized calibrated pixel value corresponding to $LMAX_\lambda$ [DN]

$LMIN_\lambda$ = Spectral at-sensor radiance that is scaled to Q_{calmin} [$W/(m^2 sr \mu m)$]

$LMAX_\lambda$ = Spectral at-sensor radiance that is scaled to Q_{calmax} [$W/(m^2 sr \mu m)$]

$G_{rescale}$ = Band-specific rescaling gain factor [$(W/(m^2 sr \mu m))/DN$]

$B_{rescale}$ = Band-specific rescaling bias factor [$W/(m^2 sr \mu m)$]

Information of this rescaling factor for Landsat data are contained in the header file (.MTL). Figure 4.2. shows an example of rescaling factors for Landsat TM image used in the study. Complete rescaling factors and radiometric calibration coefficients for all the images can be seen in Appendix C.

```
"L5109066_06620051011_MTL.txt"    CPF_FILE_NAME =
"L5CPF20051001_20051231_08"    END_GROUP =
PRODUCT_METADATA    GROUP = MIN_MAX_RADIANCE
LMAX_BAND1 = 193.000    LMIN_BAND1 = -1.520
LMAX_BAND2 = 365.000    LMIN_BAND2 = -2.840
LMAX_BAND3 = 264.000    LMIN_BAND3 = -1.170
LMAX_BAND4 = 221.000    LMIN_BAND4 = -1.510
LMAX_BAND5 = 30.200    LMIN_BAND5 = -0.370
LMAX_BAND6 = 15.303    LMIN_BAND6 = 1.238
LMAX_BAND7 = 16.500    LMIN_BAND7 = -0.150    END_GROUP
= MIN_MAX_RADIANCE    GROUP = MIN_MAX_PIXEL_VALUE
QCALMAX_BAND1 = 255.0    QCALMIN_BAND1 = 1.0
QCALMAX_BAND2 = 255.0    QCALMIN_BAND2 = 1.0
QCALMAX_BAND3 = 255.0    QCALMIN_BAND3 = 1.0
QCALMAX_BAND4 = 255.0    QCALMIN_BAND4 = 1.0
QCALMAX_BAND5 = 255.0    QCALMIN_BAND5 = 1.0
QCALMAX_BAND6 = 255.0    QCALMIN_BAND6 = 1.0
QCALMAX_BAND7 = 255.0    QCALMIN_BAND7 = 1.0
END_GROUP = MIN_MAX_PIXEL_VALUE    GROUP =
PRODUCT_PARAMETERS    CORRECTION_METHOD_GAIN_BAND1 =
"CPF"    CORRECTION_METHOD_GAIN_BAND2 = "CPF"
```

Figure 4.2. The rescaling factors contained in the product metadata of Landsat TM5 acquired on October 11, 2005.

4.1.3. Conversion to at-sensor Radiance ($L_\lambda - \rho_\lambda$)

Images acquired on different dates have different solar zenith angle, different Earth-Sun distance, and different exoatmospheric solar irradiance that arise from spectral band difference. Hence, they introduced scene-to-scene variability, which can be improved by further processing. This can be done by converting at-sensor radiance to exoatmospheric Top-of-Atmosphere (TOA) reflectance, also known as in-band planetary albedo. Chander et al. (2009) mentioned that the TOA reflectance helps remove the cosine effect of different solar zenith angle and compensates for different values of exoatmospheric solar irradiance. It also corrects for the

variation in the Earth-Sun distance between different data acquisition dates. The TOA reflectance of the Earth is computed according to the equation:

$$\rho_{\lambda} = \frac{\pi * L_{\lambda} * d^2}{ESUN_{\lambda} * \cos \theta_s} \quad (5)$$

where

ρ_{λ} = planetary TOA reflectance [unitless]

π = Mathematical constant equal to ~ 3.14159 [unitless]

L_{λ} = Spectral radiance at the sensor's aperture [$W/m^2 sr \mu m$]

d = Earth-Sun distance [astronomical units]

$ESUN_{\lambda}$ = Mean exoatmospheric solar irradiance [$W/m^2 sr \mu m$]

θ_s = Solar zenith angle [degrees]

4.1.4. Atmospheric correction by Dark-Object Subtraction (DOS)

The atmosphere affects images by scattering, absorbing, and refracting light and these effects are wavelength dependent. Several methods are available to correct for this effect including the Dark-Object Subtraction (DOS) technique. The DOS atmospheric correction is an image-based technique, hence it does not require an in-situ measurement during the acquisition of satellite images (Chavez, 1988; Chavez, 1996). This technique assumes that there is high probability that there are at least a few pixels within an image which should be black (0% reflectance), for example, areas of shadow caused by topography or clouds in the image where the pixels should be completely dark. Ideally, an imaging system should not detect radiance at these shadow locations, and a DN value of zero should be assigned to them. However, because of the atmospheric scattering effect, these shadowed areas will not be completely dark and the sensor records a non-zero DN at these locations. The value of DN at this location is assumed to be the *haze* value and needs to be subtracted from the particular band to account for atmospheric scattering effect. Chavez (1996) also states the fact that there is only a few objects

on the Earth's surface that are completely dark and so an assumption needs to be made that these objects have at least one-percent of reflectance.

Therefore assuming that there are some dark objects whose reflectance are supposed to be around zero, then the minimum DN value need to be subtracted from all the pixels so that atmospheric effect can be removed from the entire image.

Sobrino et al. (2004) express the path radiance (atmospheric scattering) as:

$$L_p = L_{min} - L_{1\%} \quad (6)$$

Where

L_{min} is radiance that corresponds to a DN value for which the sum of all pixels with DN value lower or equal to this value is equal to the 0.01% of all the pixels from the image considered (Sobrino et al., 2004, p.437). This radiance value can be obtained using equation 4.

$L_{1\%}$ is the radiance of dark object assumed to have reflectance value of 0.01.

Therefore, L_{min} and $L_{1\%}$ can be expressed like the following:

$$L_{min} = G_{rescale} * DN_{min} + B_{rescale} \quad (7)$$

$$L_{1\%} = 0.01 * [(ESUN_{\lambda} * Cos\theta_s * TAU_z) + E_{down}] * TAU_v / (\pi d^2) \quad (8)$$

And the path radiance can be obtained by substituting equations 7 and 8 into equation 6:

$$L_p = G_{rescale} * DN_{min} + B_{rescale} - 0.01 * [(ESUN_{\lambda} * Cos\theta_s * TAU_z) + E_{down}] * TAU_v / (\pi d^2) \quad (9)$$

Chavez (1996) computed the variables TAU_z , TAU_v and E_{down} to be the following:

$$TAU_z = 1$$

$$TAU_v = 1$$

$$E_{down} = 0$$

This is assuming the no atmospheric transmittance loss, and corrects for the spectral band solar irradiance and solar zenith angle, resulting in:

So, by substituting these values into equation 9, the path radiance (atmospheric scattering) can be obtained by:

$$L_p = G_{rescale} * DN_{min} + B_{rescale} - 0.01 * ESUN_{\lambda} * Cos\theta_s / (\pi d^2) \quad (10)$$

Finally, to obtain the surface reflectance of Landsat images equation 10 is substituted into equation 5 as expressed below:

$$\rho_{\lambda} = \frac{[\pi * (L_{\lambda} - L_p * d^2)]}{ESUN_{\lambda} * cos\theta_s} \quad (11)$$

Where L_{λ} is defined by equation 4, L_p is defined by equation 10, d is the Earth-Sun distance in astronomical units. $ESUN_{\lambda}$ is obtained from Chander et al. (2009) and $cos\theta_s$ is the cosine of solar zenith angle θ_s reported in the images metadata file. The reflectance value should range between 0 and 1 and so values below and above this range were corrected. Any reflectance value below 0 was set to 0 and any reflectance value higher than 1 was set to 1. All the raw data used in this study were converted into radiance, reflectance and atmospherically corrected. Hence, they were comparable even though they were captured by different sensors at different times.

4.1.5. Classification scheme

In this study, a modified land use/class scheme, based on the Anderson's scheme level I and II (Anderson et al., 1976), the proposed land cover classes by the Ministry of Fisheries and Agriculture of East Timor (MAF, 2001) and the author's a priori knowledge of the study area were used to defined land cover classes in the study area. In total seven land use/cover classes were considered in this study. Description of these categories is listed below:

Forest. This class includes forested land that exists throughout the study area. Coniferous and deciduous forest belongs to this category. Coastal forest such as thick mangrove is also included in this category. This class was easily discriminated using False Color Composite of 432 and 542 of Landsat images.

Mixed Rangeland: This class comprises of sparse woodland or scattered trees. Shrubs are also included in this class

Grassland: This category includes savanna and land used for grazing.

Farmland: This class primarily consists of lands used permanently for food production both commercial and non-commercial purposes. Rice fields, plantations, and non-irrigated land belong to this class.

Settlements: This class includes small towns, villages, roads, airports and concrete structure, as identified by visual interpretation on the satellite images.

Bare soil: This class consists of barren land, bare rocks, and soil that are exposed due to the burning of trees, and shifting cultivation. Note that farmland that is dry are not included in this class.

Water: Lakes and rivers.

4.2. Image Processing

Image processing involves the manipulation and interpretation of digital images using computers (Lillesand et al., 2004). This step is performed in this study to differentiate forest cover among other covers for change detection. This is achieved through a combination of Normalized Difference Vegetation Index (NDVI) differencing and image classification. The following section explains these two methods.

4.2.1. Normalized Difference Vegetation Index (NDVI)

In the image processing phase, an NDVI differencing technique is applied to identify pixels that change and don't change between two different dates. The NDVI is derived from the red – near infrared reflectance ratio. The formula is based on the notion that that chlorophyll accumulating within leaves of healthy green vegetation absorb red wavelengths, whereas the mesophyll leaf structures and water within the leaf scatter near infrared. NDVI values, which are unitless, range from –1 to +1, where positive values yield high amounts of vegetation, both deciduous and otherwise, where negative values correspond to sparse or nonexistent vegetation, bare soil and clouds. For Landsat TM and ETM+, NDVI is defined by $\text{band4} - \text{band3} / \text{band4} + \text{band3}$, whereas for Landsat MSS, it is defined as $\text{band4} - \text{band2} / \text{band4} + \text{band2}$ (Jensen, 2005)

NDVI differencing is a widely used technique in change detection studies (Masek et al., 2000,; Pu et al., 2008). Although Pu et al. (2008) used a linear model to perform normalization between images to account for radiometric differences between images, this was not necessary in this study because radiometric and atmospheric correction have been performed in the previous phase. Thus all the images were comparable to each other.

After calculating NDVI for all the years, the difference between NDVI of one observation date to NDVI of another date was calculated to identify pixels that change and don't change. This was performed by subtracting NDVI 1972 from NDVI 1987 to obtain changes between NDVI of these two dates. Similarly, NDVI 1987 was subtracted from NDVI 1996, NDVI 1996 from NDVI 2000, NDVI 2000 from NDVI 2005, and NDVI 2005 from NDVI 2011 to generate NDVI differences between those two image pairs.

Next, the NDVI differencing images were further processed by splitting pixels distribution above and below the mean into two parts, the decrease (L_L) and increase parts (L_H) (See Figure 4.2.1. for L_L and L_H). Pixels with values above the mean of NDVI differencing image were treated as the index decrease part and pixels above the mean of the NDVI differencing image were treated as index increase part. Next, the mean (m_d and m_i) and standard deviation (s_d and s_i) for these two images were identified, where subscript d represents index decrease part and i represents index increase part (Pu et al., 2008). Pixels that change in the index decrease part were obtained by identifying their values that fall below $m_d + Cs_d$, and pixels that change in the index increase part were obtained by identifying their values that fall above $m_i - Cs_i$.

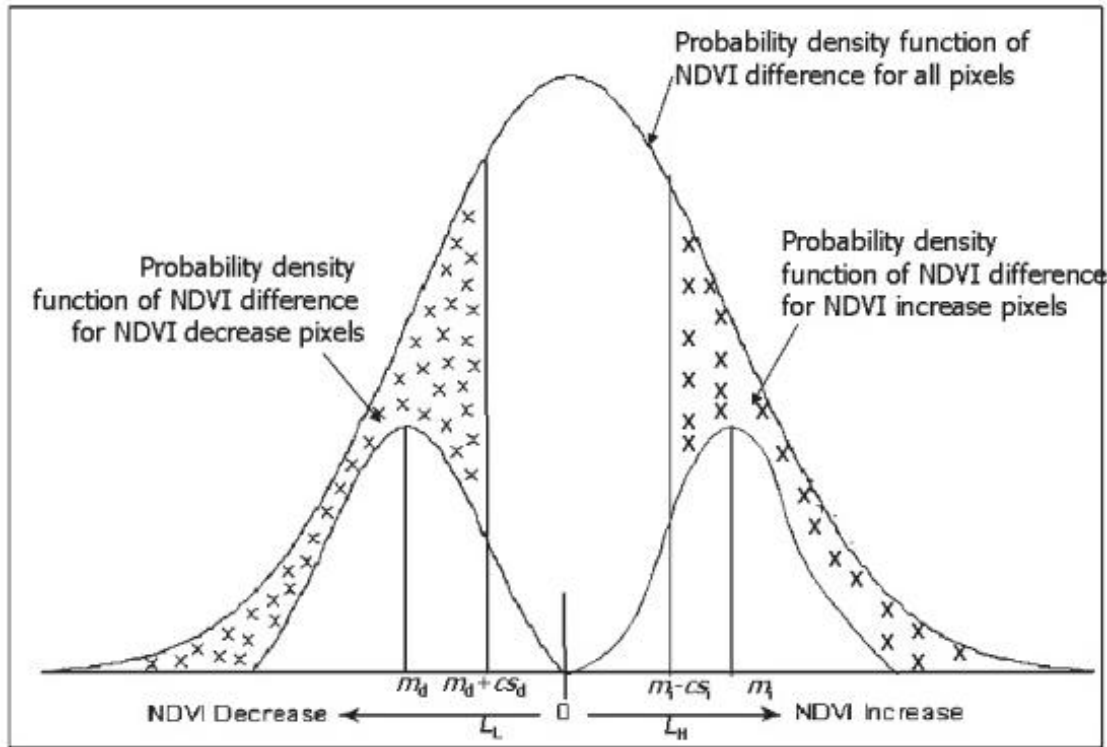


Figure 4.2.1. Probability density function of NDVI differencing image. Source: Pu et al. (2008)

The c refers to a range of coefficient (values between -1.8 and 0.4) that can be used to calculate different thresholds to show the best change/no change (Figure 4.2.1.1). Ideally, the optimum c to determine threshold values is computed using

Kappa or other accuracy indices (Pu et al., 2008). However, due to the lack of ground-truth data, the threshold values were determined by visually inspecting maps that were produced using different coefficients. The visual inspection reveals that as c increases (small negative value) a lot of noise is introduced but information is lost as the value of c decreases (larger negative value). Hence, the optimum threshold values is found to be in the range of -0.6 and -0.2.

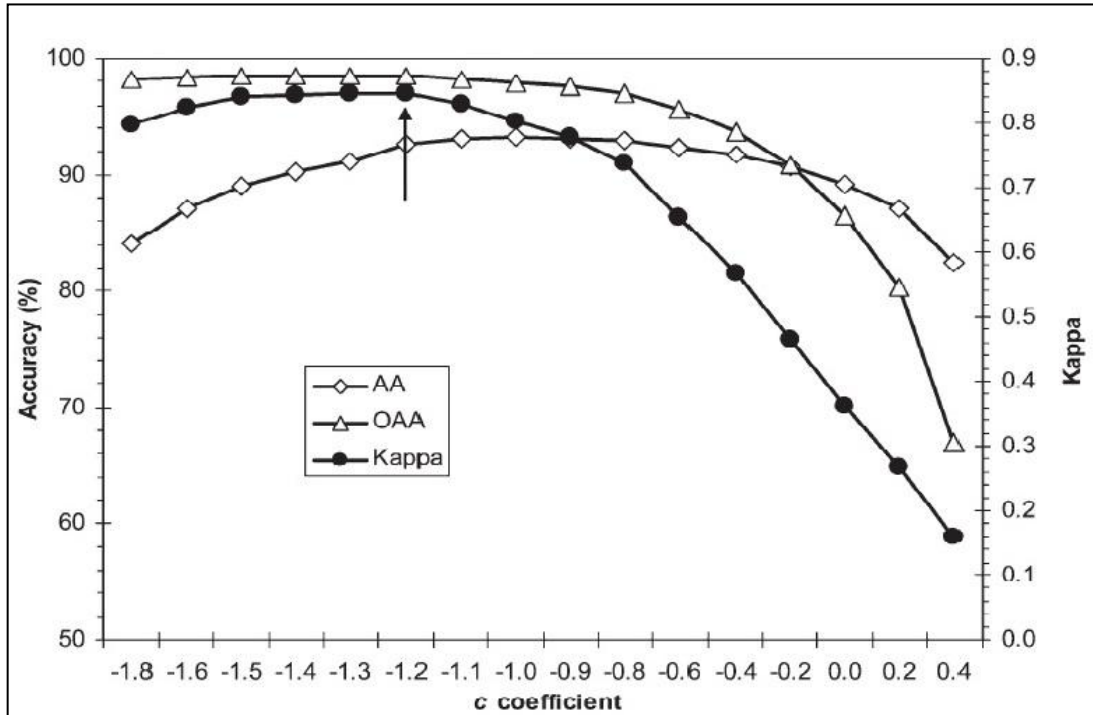


Figure 4.2.1.1. Range of optimal c value. Source: Pu et al. (2008)

4.2.2. Image Classification

The next step in the image processing phase is image classification. Two types of classification algorithms were employed, Maximum Likelihood (MLC) and Isodata Cluster. The MLC is an algorithm that quantitatively classifies pixels by evaluating both the variance and covariance of the categorical spectral response pattern (Lillesand et al., 2004). This is based on the assumption that similar features with similar spectral signature have a normal distribution and their statistical probability can be computed. It is a technique of supervised classification being

that the analyst defines training areas to train the algorithm, which then classify pixels based on their likelihood to belong to the defined class (CCRS, n.d.).

Isodata cluster is a method of unsupervised classification that works by iteratively grouping cells into a user-defined number of distinct unimodal class (ESRI, 2010). The algorithm starts by arbitrarily assigning means (center) to cluster to which each cell with minimum distance belong. After the first iteration, the means are recalculated until the maximum number of iteration is reached.

The MLC was used to classify the year 2000 image which serves as reference image for all the other images. A total of 100 samples were collected for forest, 100 samples for mixed rangeland, 100 for farmland and 50 samples for bare soil. For built-up areas, grassland and water, 50 classes were collected for each of them. These samples were collected by visually interpreting the 2000 image using False and True color composites. After the classification an accuracy assessment was performed on the classified image of 2000 using the 2001 topographic and land use map as reference data from which samples were collected.

Congalton and Green (2008) stated that the general guideline “rule of thumb” regarding the sample size for of an accuracy assessment is to collect 50 samples for each class in a map that has a size of less than a million hectare and less than 12 classes. For a much larger map, they suggested 75 to 100 samples points per class as this will ensure a balance between statistical validity and practicality (Congalton and Green, 2008, p.75). Hence, in this study, a total of 700 points were randomly collected from the image for the purpose of an accuracy assessment. This one time accuracy assessment is necessary not only because it is a fundamental requirement in a change detection study but also because the 2000 map serves as the reference for all the other observation dates.

For all the other images, the unsupervised classification with ISO Cluster algorithm was employed by assigning 30 classes. The clusters of pixels were then grouped based on the defined land use/cover categories. Interpretation of RGB images by False Color Composite (FCC) and True Color Composite (TCC) from each observation date was performed to assist in the assignment of the classes.

The final classification maps were obtained by combining change/no change maps generated by NDVI differencing and maps generated from both supervised and unsupervised classification (see Figure 4.2.2). Afterwards, a 3 x 3 pixels majority filter was applied to all the classified maps to remove some of the speckled pattern (noise) of individual pixels.

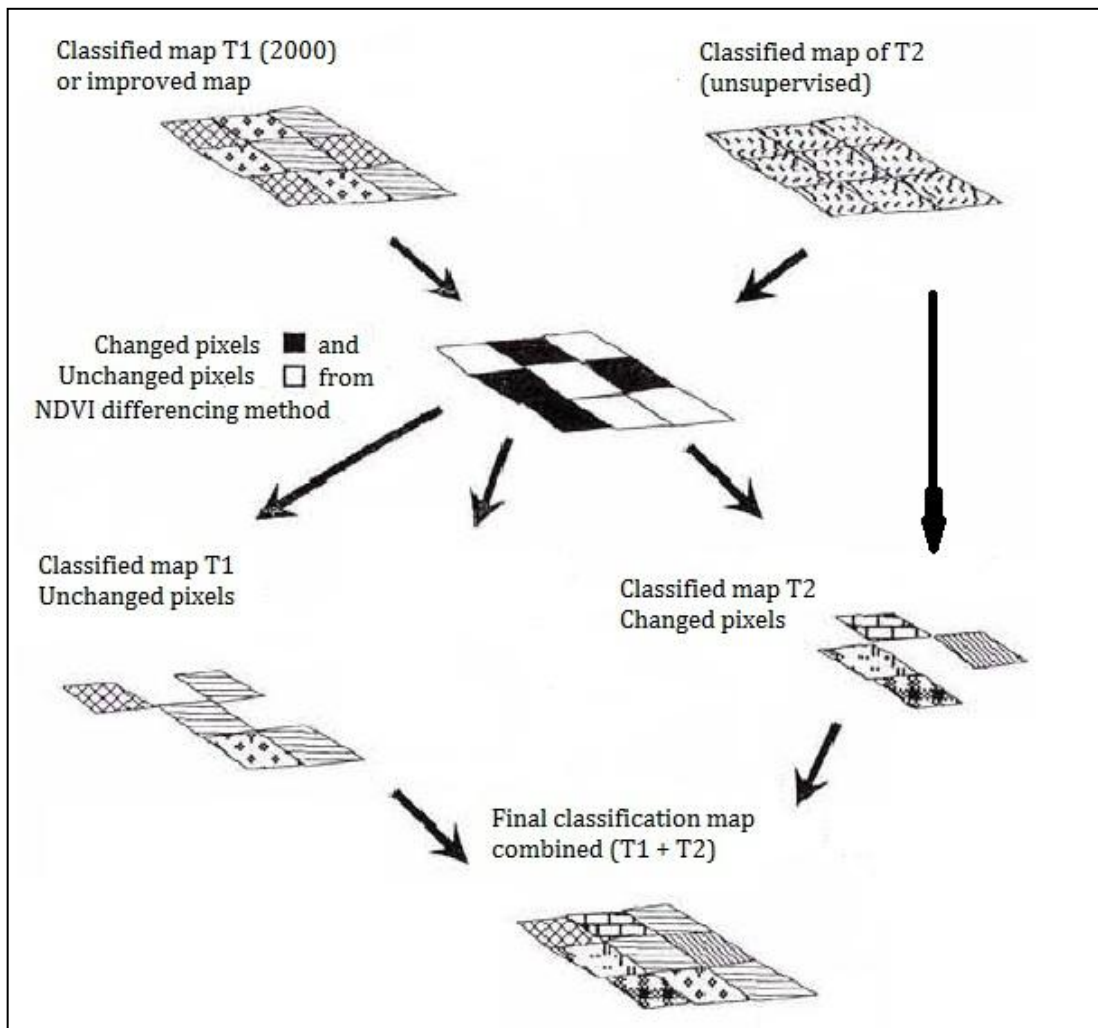


Figure 4.2.2. Derivation of final classification maps for five acquisition dates (1972, 1987, 1996, 2005 and 2005) by combining change/no change maps and classified maps from supervised and unsupervised methods



4.2.3. Change rationality test

To improve the final classification maps, it is necessary to understand whether or not some of the changes between pixels make sense. For instance, it is unlikely that built-up areas will change into forested land or farmland. Additionally, in tropical region such as East Timor, where deforestation occurs due primarily to shifting cultivation and expansion of farmland, change from farmland or bare soil to forest is very unlikely. Therefore, a rule can be established to assess the rationality of

changes between pixels. The following four rules have been used to perform this assessment.

Let x be the number of detected categorical changes over six monitoring dates (1972–2011).

$$0 \leq x \leq 5$$

where $x = 0$ means no change at all, and $x = 5$ means that the pixel of the cover type has undergone changes through every detection period. Consider also that  = a specific cover type and  = a different cover type and T1 – T6 refers to six observation dates.

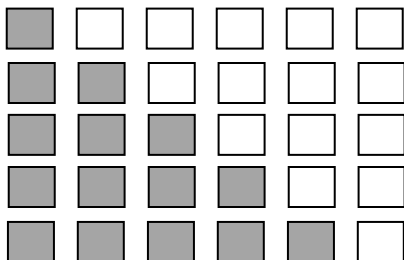
Rule I: no change ($x = 0$), if a pixel is classified as the same land cover type throughout the six monitoring periods then it is ‘correctly’ classified.


T1 T2 T3 T4 T5 T6



      Correct for all cover types.

      Correct for all cover types.

Rule II: One-time change ($x = 1$), if a pixel changes from one cover type to a different cover type for once, and once only, then it is classified as correct. However, there is an exception to pixels with cover type built-up area, bare soil and farmland. If a pixel is found to have changed from built-up area to different cover type, it is considered as a ‘reverse’ case and is classified as ‘incorrect’. In that case, the pixel failed Rule II and needs to be passed to the next test. Similarly, a change of pixel with cover type farmland or bare soil to forest is also considered ‘incorrect.’



Correct; incorrect if  = built-up areas

Correct; incorrect if  = farmland / bare soil,
 = forest

Rule III: ‘The rule of majority’, a pixel is considered majority class if it is classified as the same cover type for four times or more, irrespective of their order in between T1 and T6. This pixel is considered correct and the other two pixels that are incorrect will be reclassified similar to the correct one.



Rule IV: this rule deals with all the pixels that failed all the previous tests above ($x > 2$). Pixels in this category are those that change multiple times between cover types but don’t retain majority. For example, a pixel in 1972 may be classified as forest, but grassland in 1987 and built-up in 2000. It is difficult to know whether or not this is a true land cover change and so they are considered ‘fuzzy’ pixels. Pixels in this category will be reclassified based on the information from 2000 image because this is the only reliable map.

4.3. Post-classification change detection

After the final maps are reclassified and improved through change rationality test, a post-classification comparison is performed to detect LULC change. This technique performs change detection in which comparison is made between independently classified images (Singh, 1989). Post classification comparison has the advantage to provide direct information on the nature of land cover change. To perform the change detection two maps were paired to calculate their categorical change. For instance, the map of 1972 was paired with 1987 to calculate how much of an area of a class in 1972 map had changed in the map of 1987. This procedure was performed in ArcGIS using the function ‘Tabulate Area’.

CHAPTER 5

RESULTS AND DISCUSSION

5.1.NDVI

The NDVI calculations were obtained for all the observation dates (Figure 5.1.1). Visual analysis of the images shows that large proportions of healthy vegetation were located mostly in southern region of the study area. Toward the northern region, NDVI shows relatively low values. In 1972, however, high NDVI values were observed primarily in the western part of the study area. This is contrary to the distribution of vegetation in 1987 where higher NDVI values shifted toward the eastern part of the island. Although from 1996 on, the INDVI map looks fairly similar, it's apparent that the 2005 map shows less greenness compared to all other maps. See Appendix D for enlarged version of NDVI images.

5.2.NDVI Differencing

The results from NDVI differencing techniques were obtained for all the observation dates. After conducting visual inspection of NDVI differencing images with different c coefficients, the optimal threshold values for change/no change were determined. The change/no change map were generated using the optimum threshold values ranging from -0.6 to 0.2 (see Appendix A for change/no change maps). Table 5.2.1 shows the mean, standard deviation, and optimum threshold values for all the image pairs

NDVI Differencing	Index Decrease		Index Increase		Optimum c value	Threshold	
	Mean	SD	Mean	SD		Decrease	Increase
1972 – 1987	-0.662	0.323	-0.057	0.155	- 0.6	0.4682	0.036
1972 – 1996	0.001	0.187	0.456	0.291	-0.2	-0.0384	0.5142
1996 – 2000	-0.021	0.180	0.253	0.210	-0.2	-0.057	0.295
2000 – 2005	-0.569	0.197	-0.192	0.177	-0.6	-0.6872	-0.0858
2005 – 2011	0.142	0.176	0.547	0.200	-0.6	0.034	0.667

Table 5.2.1. Thresholds of index decrease and increase for all NDVI differencing images

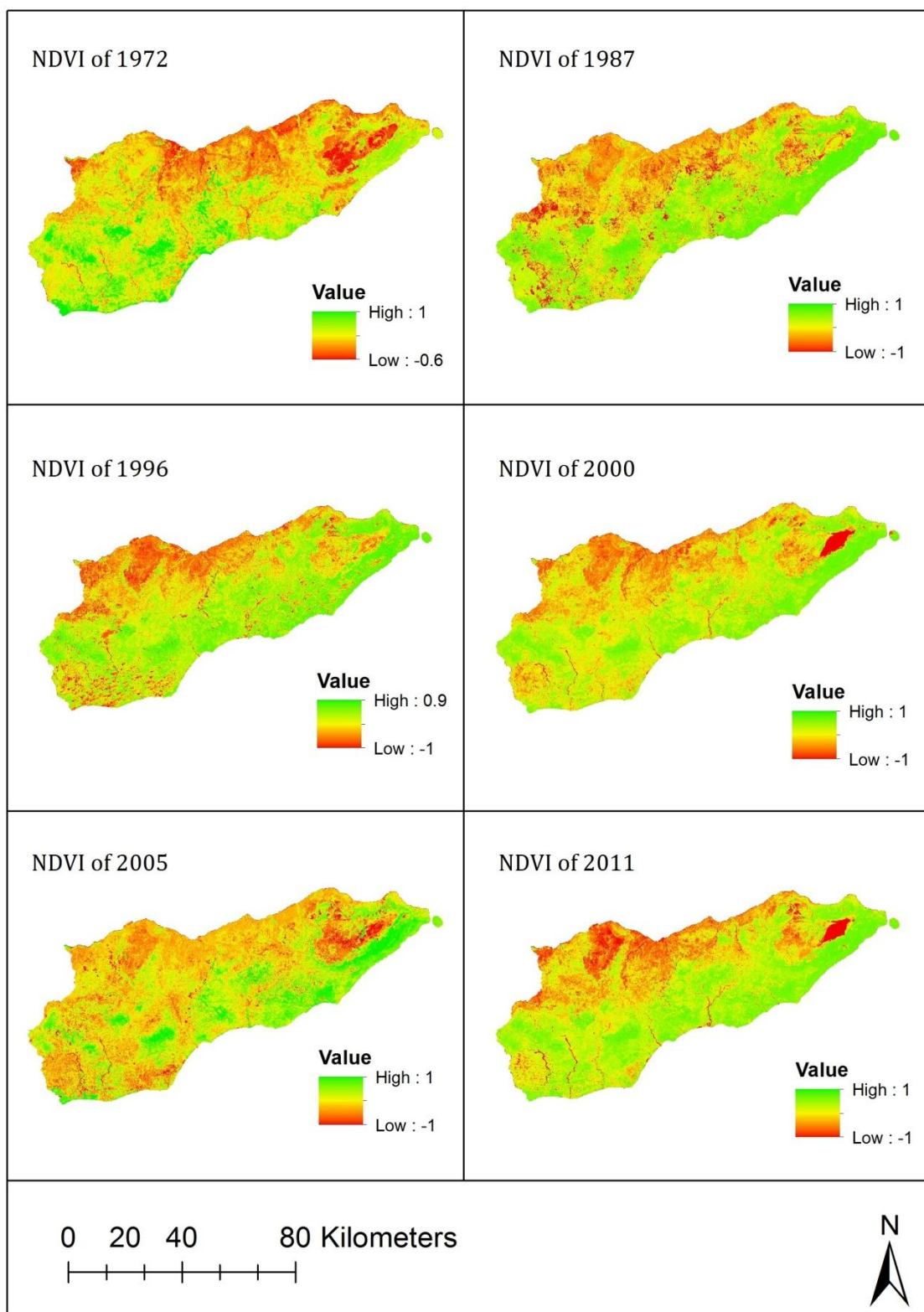


Figure 5.1.1. NDVI maps for all observation dates

5.3. Selection of coefficients

Ideally, selection of the optimum threshold value is done by measuring its performance against some accuracy indices. However, due to the lack of ground data (reference data) in this study the selection of the optimum threshold value were done by visual inspection of each map generated using all the different c values. One of the techniques used in this study is by observing features in the image that is assumed to have a constant low (or high) index value throughout the study period and using it as a basis for helping in determining the threshold value. For instance, feature such as airport rarely changes for long period of time and so the difference value for pixels around this area should be close to zero either above or below the mean. The c values for both the index decrease and increase parts were arbitrarily chosen so that they don't include pixels that contain the feature's information (Figure 5.3.1). Pixels of other features, assumed to have relatively constant zero value, were also used as indicators. Hence, the threshold values were selected by distinguishing true change (larger negative value) from noise (lower negative value).

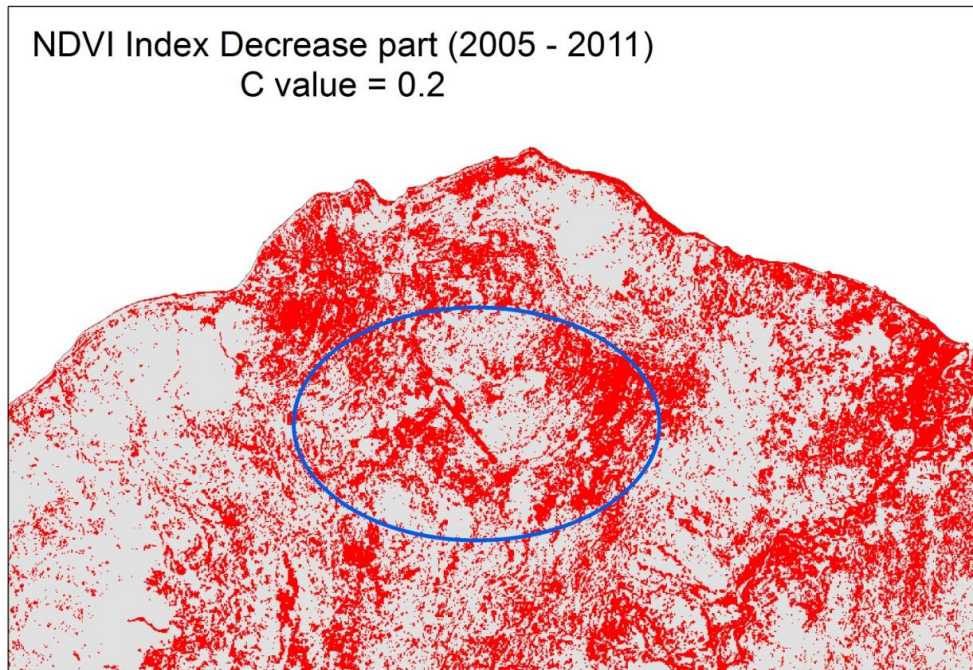


Figure 5.3.1. NDVI index decrease part shows large amount of noises due the selection of high c value (smaller negative). The blue circle shows and airport runway

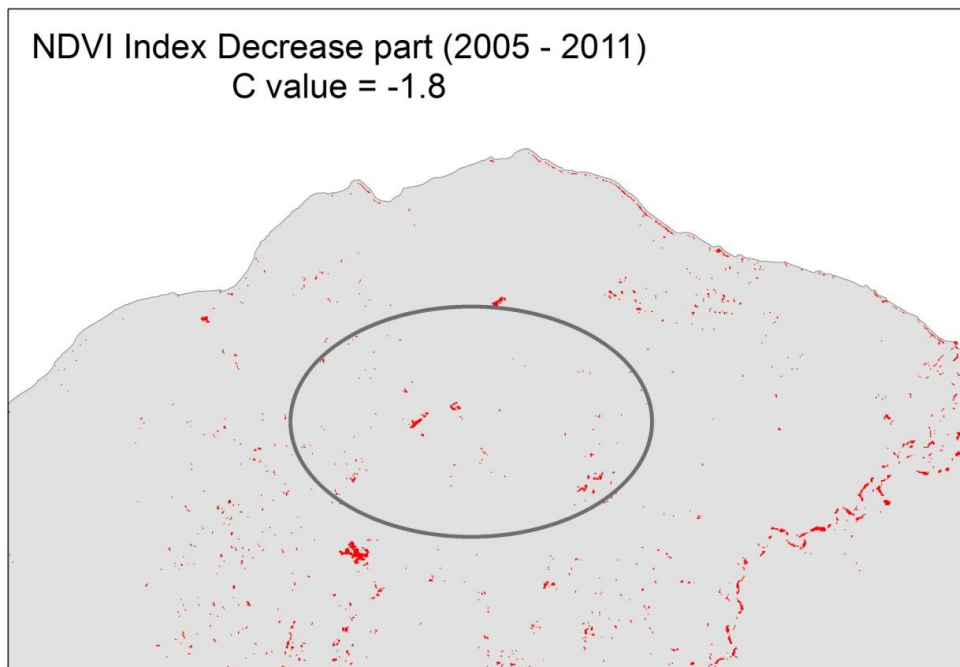


Figure 5.3.2. NDVI index decrease part shows minimum noise due to selection of low c value (larger negative).

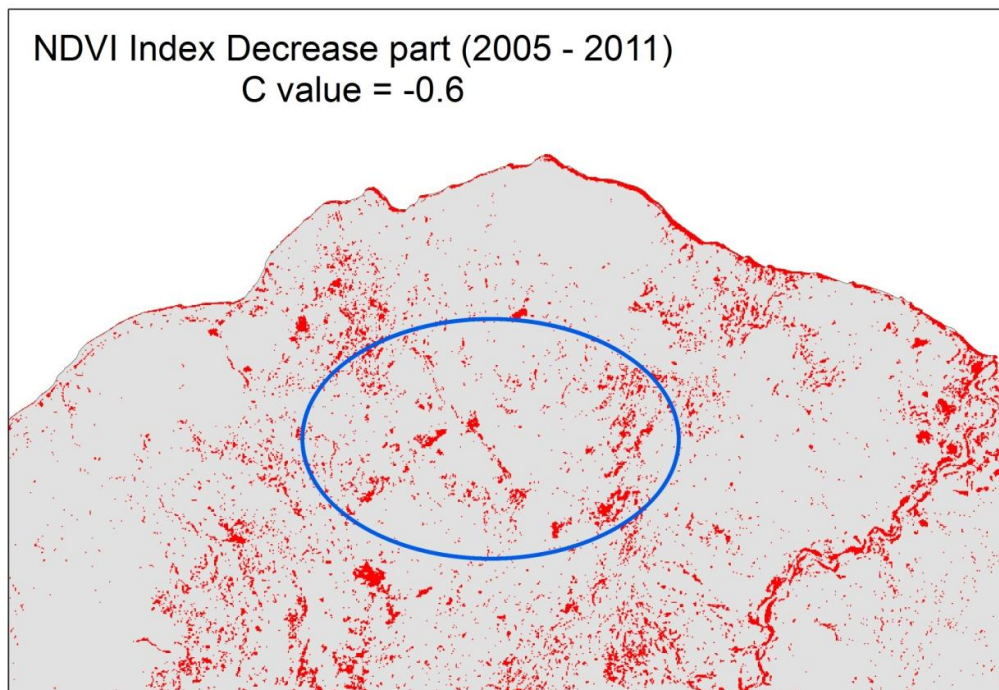


Figure 5.3.3. NDVI index decrease part using medium c value. Notice the reduction in the noise but enough change information are retained.

5.4. Image classification

Conducting an accuracy assessment for a classified image is necessary especially if the image is to be used for further analysis. It is particularly important in post-classification change detection analysis where the accuracy of the final change image depends on the accuracy of the independently classified images (Yuan et al., 2005). In determining the accuracy of this image, 700 sample points were randomly distributed across the study area. The different land use/cover categories in the classified image were compared with the topographic map and land use map of East Timor for the year of 2000 by using the confusion matrix. The result shows an overall accuracy of 0.82% with a kappa index of 0.77 (Table 5.3.1). As mentioned in the methodology section, after conducting accuracy assessment, the 2000 map was used to classify images from other years for which NDVI differencing identified as no change. For pixels that NDVI differencing identified as change, they were classified using unsupervised method. Finally, these maps were improved by applying change rationality test.

Categories	Producer accuracy (%)	User accuracy (%)
Forest	90	82
Mixed Rangeland	83	86
Grassland	83	84
Farmland	74	82
Settlement	52	57
Bare soil	78	73
Water	86	86

Table 5.3.1. One time accuracy assessment for 2000 image

5.4.1. Change rationality test: Rule I

The change rationality test over the six-time multi-temporal image classification results are divided into four steps, Rule I, II, III and IV. Rule I provide an initial

assessment of the LULC change rationality by separating change and no change pixels throughout the six observation dates. First it identifies pixels that don't change and labels them as 'correctly' classified, and 'uncertain' for pixels that change. Of the total 5572060 pixels, 3072292 pixels remained unchanged throughout the six observation dates, accounting for 55% of the total pixels (Table 5.4.1.1). From these unchanged pixels, forest constitutes 1095588 number of pixels, about 20% of the total, and mixed rangeland constitutes around 33%. All other cover types together only make up about 2% of the total pixels (Figure 5.4.1.1)

	Forest	Mixed Rangeland	Grassland	Farmland	Built-up	Bare soil	Water
Unchanged Pixels	1095588	1856754	99048	15578	1356	3272	696

Table 5.4.1.1. Total number of unchanged pixels for each category as defined by Rule I

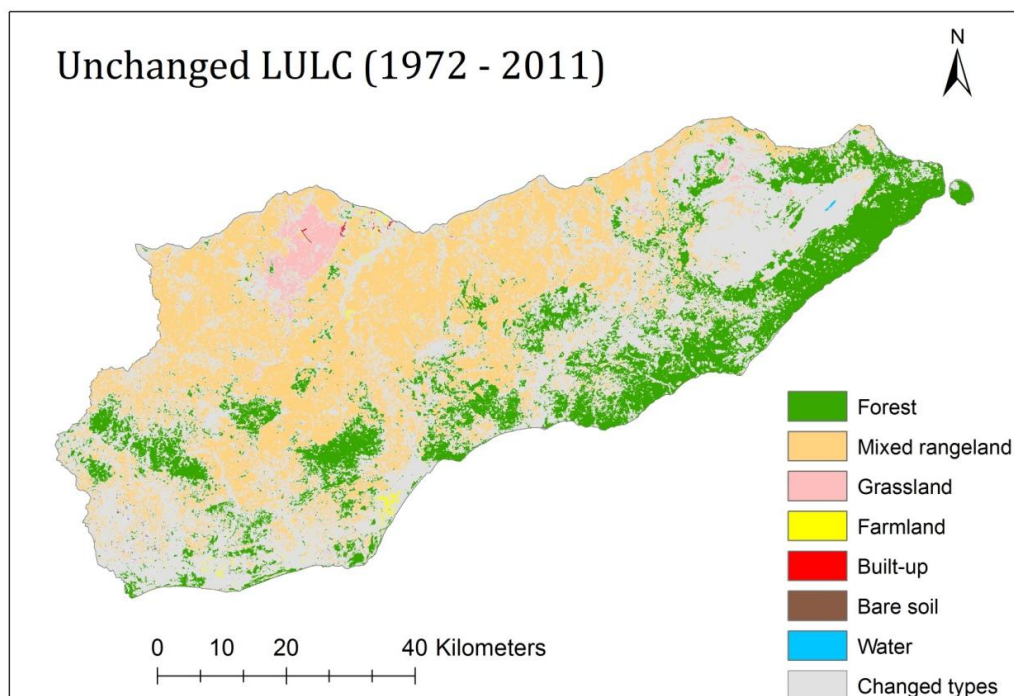


Figure 5.4.1.1. Unchanged LULC categories between 1972 and 2011 as identified by change rationality test

5.4.2. Change rationality test: Rule II

The objective of Rule II is to test for true land cover change by identifying once-only change that occur between two cover types with the exception of change from built-up areas to different cover type and change from farmland or bare soil to forest. Of the total 3072292 pixels that changed between 1972 and 2011, 1794360 pixels were identified as change between one cover type to a different cover type, leaving 1277932 pixels to be tested further. The largest change identified by this Rule was from forest to mixed rangeland (458210 pixels).

5.4.3. Change rationality test: Rule III and Rule IV

The Rule III use the 'rule of majority' to identify pixels of one cover type that occur four or more times throughout the six monitoring dates and then label it as the correct class for all the monitoring dates. The incorrect pixels were than reclassified as the majority pixels. 703799 pixels were identified in this test. The remaining 1609 pixels were considered 'uncertain' because they change multiple times (more than two times) and no single class retain majority. Each of these pixels were reclassified as the class in the map of 2000. The result of change rationality test is summarized in Table 5.4.3.

Rules	Number of Pixels	(proportion to the total pixels)
Rule I	3072292	0.55
Rule II	1794360	0.32
Rule III	703799	0.12
Rule IV	1609	0.0002
Total	5572060	1.00

Table 5.4.3. Summary of change rationality test

5.5. Post-classification comparison

The final improved classification maps have been obtained (See appendix B). Individual class and its proportion to total area for the six observation dates are summarized in Table 5.5.1 and Table 5.5.2 respectively. It can be seen from Table 5.5.2 and Figure 5.5.1 that the study area is predominantly covered with mixed rangeland. This class occupies more than half of the total area throughout the six monitoring dates. Forest is the second largest LULC category covering 34% of the total area in 1972, but eventually dropped to 28% in 2011. In 1972, bare soil was the third largest LULC category in the study area (11.7%). However, since 1987 increase in farmland makes it the third largest category. Apparently between 1972 and 2011 forested land was reduced by 29000 ha (6%) while grassland decreased by 12000 ha (2%). Relatively, built-up areas increased approximately by 1282.23 ha while farmland, mixed rangeland, bare soil and water increased by 16000 ha, 15000 ha, 7000 ha and 1000 ha respectively. The result of this post-classification comparison is detailed below.

LULC Categories	1972 (000 ha)	1987 (000 ha)	1996 (000 ha)	2000 (000 ha)	2005 (000 ha)	2011 (000 ha)
Forest	169.8	149.1	148.2	147.3	145.6	140.7
Mixed Rangeland	250.1	274.4	274.9	273.6	263.2	265.2
Grassland	50.6	33.9	33.9	33.8	38.4	38.6
Farmland	9.6	21.0	21.1	22.3	24.8	25.9
Built-up	4.3	4.3	4.4	4.6	4.9	5.5
Bare soil	11.7	13.1	13.2	13.9	18.5	19.1
Water	5.4	5.7	5.7	6.0	6.1	6.4

Table 5.5.1. Summary of final classification map area statistics for six observation dates

LULC Categories	1972 (%)	1987 (%)	1996 (%)	2000 (%)	2005 (%)	2011 (%)
Forest	0.34	0.30	0.30	0.29	0.29	0.28
Mixed Rangeland	0.50	0.55	0.55	0.55	0.52	0.53
Grassland	0.10	0.07	0.07	0.07	0.08	0.08
Farmland	0.02	0.04	0.04	0.04	0.05	0.05
Built-up	0.008	0.009	0.009	0.009	0.010	0.011
Bare soil	0.023	0.026	0.026	0.028	0.037	0.038
Water	0.011	0.011	0.011	0.012	0.012	0.013

Table 5.5.2. The percentage of land use categories for each observation date

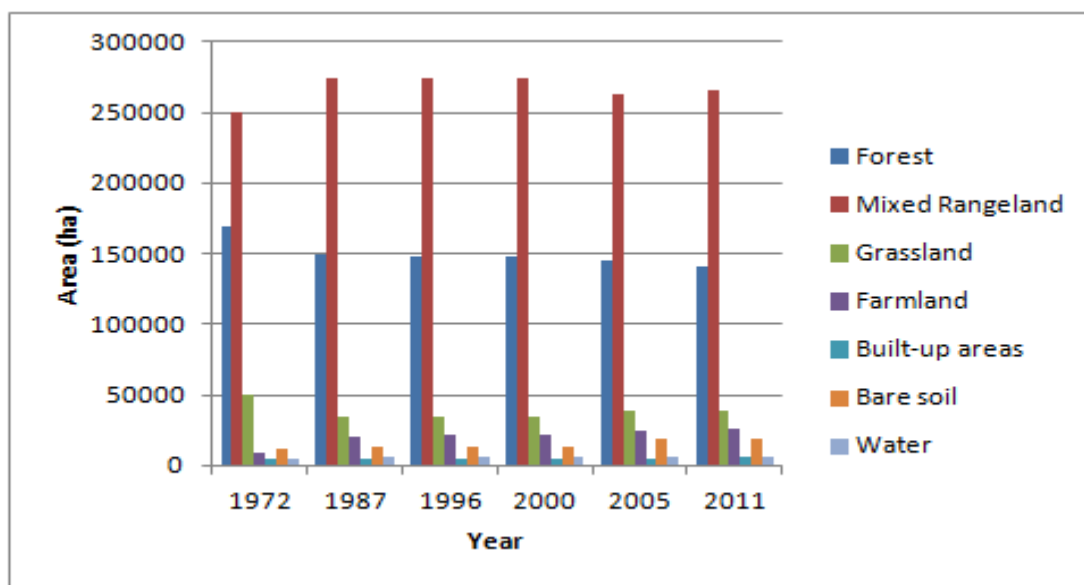


Figure 5.5.1. Distribution of land cover types in East Timor between 1972 and 2011

5.6. Post-classification change detection

To further evaluate the results of land cover change, matrices of land cover changes from 1972 to 1987, 1987 to 1996, 1996 to 2000, 2000 to 2005, 2005 to 2011, and 1972 to 2011 were created (Table 5.6.1, Table 5.6.2, Table 5.6.3, Table 5.6.4, Table 5.6.5). The matrix is read from left to right and showing the amount of area change (hectare) from one observation date to the next observation date. For instance, Table 5.5.3 shows LULC categories in 1972 that changed in 1987. The major diagonal matrix shows land cover categories in 1972 that remained the same in 1987, that is, the unchanged class.

1972	1987 (Area in ha)						
	Forest	Mixed rangeland	Grassland	Farmland	Built-up	Bare soil	Water
Forest	124042.32	41238.9	1402.11	2358.18	83.34	626.94	74.43
Mixed Rangeland	23611.05	208615.6	3893.4	8815.14	0	4615.38	546.03
Grassland	1050.12	20816.01	28306.89	98.37	0	332.1	12.6
Farmland	0	0	129.96	9452.97	0	0	0
Built-up	0	0	0	0	4255.29	0	0
Soil	0	3767.04	184.14	230.67	6.3	7504.11	7.83
Water	360.72	0	0	0	0	0	5047.47

Table 5.6.1. Matrix of land cover change from 1972 to 1987

Table 5.6.1 shows that 41238.9 hectares of forest changed into mixed rangeland and 4470.57 hectares of it were converted into grassland, farmland, built-up areas and bare soil altogether. Although, mixed rangeland also changed to forest (23611.05 ha), a significant amount of it were converted into grassland, farmland and bare soil (17323.92 ha). These changes may seem to be classification errors, but forested areas are among some of the most extracted areas in East Timor for firewood and timbers. In addition, considering the time interval of 15 years, these changes are likely to occur.

1987	1996 (Area in ha)						
	Forest	Mixed rangeland	Grassland	Farmland	Built-up	Bare soil	Water
Forest	148009.77	1004.22	0.09	19.8	9.45	6.57	14.31
Mixed Rangeland	190.53	273786.6	47.7	156.42	75.15	148.86	32.31
Grassland	0.09	68.58	33832.44	0	15.39	0	0
Farmland	0	8.28	0	20943.36	0.81	2.34	0.54
Built-up	0	0	0	0	4344.84	0.09	0
Soil	0	10.44	0.09	3.6	0	13064.31	0.09
Water	0	0	0	0	0	0	5688.36

Table 5.6.2. Matrix of land cover change from 1987 to 1996

Compared to 1972 and 1987, the reduction of forest from 1987 to 1996 was actually lower. Between 1987 and 1996 1004.22 ha of forest changed into mixed rangeland and only 35 ha were actually converted into grassland, farmland, built-up areas and bare soil (Table 5.6.2). However, there was 428 ha conversion of mixed rangeland into grassland, farmland, built-up areas and bare soil. This is in contrast to the period between 1996 and 2000 where 1895 ha of mixed rangeland changed into grassland, farmland, built-up and bare soil class (Table 5.6.3.) Approximately 225 ha of this class also changed into water. This might also seem to be classification error but visualization of satellite images confirmed that there was unusual high water level at lake “Iralalaru” during this period. For the period between 1990 and 2000, approximately 117 ha of forest areas were converted into farmland, 10 ha into built-up areas, 13 ha into grassland and 27 ha into bare soil.

1996	2000 (Area in ha)						
	Forest	Mixed rangeland	Grassland	Farmland	Built-up	Bare soil	Water
Forest	146489.76	1537.02	13.14	117.72	10.17	27	5.58
Mixed Rangeland	822.78	271934.9	29.7	1035.45	161.46	668.52	225.27
Grassland	2.61	114.48	33759.63	0.63	0	2.97	0
Farmland	0	0	0	21084.75	0	30.6	7.83
Built-up	0	0	0	0	4445.64	0	0
Bare soil	0	36.36	0.09	26.64	0.72	13157.73	0.63
Water	0	0	0	0	0	0	5735.61

Table 5.6.3. Matrix of land cover change from 1996 to 2000

Reduction in forest area continued to occur after the year 2000. As shown in Table 5.6.4, more than 800 hectares of forest land were converted into grassland, farmland, built-up areas and bare soil. This amount, however, is still lower than the amount of mixed rangeland that were converted into farmland alone (2259 ha) in the same period. The largest change in this period was the conversion of mixed rangeland into bare soil (4538 ha).

2000	2005 (Area in ha)						
	Forest	Mixed rangeland	Grassland	Farmland	Built-up	Bare soil	Water
Forest	143920.89	2535.84	249.3	292.41	31.14	279.99	5.58
Mixed Rangeland	1498.86	260431.8	4472.55	2259.99	283.5	4538.88	137.16
Grassland	130.59	28.71	33625.35	11.25	6.66	0	0
Farmland	0	69.3	0	22178.16	10.17	0	7.56
Built-up	0	0	0	0	4617.99	0	0
Soil	0	169.83	19.26	53.01	0.36	13642.74	1.62
Water	0	0	0	0	0	0	5974.92

Table 5.6.4. Matrix of land cover change from 2000 to 2005

The period between 2005 and 2011 witnessed a conversion of more than 4000 hectares of forest land into mixed rangeland (Table 5.6.5). In addition, more than 800 hectares of forest also changed into farmland, grassland, built-up areas and bare soil. During this period conversion of mixed rangeland is much lower than the previous observation date (2000 – 2005). As shown in Table 5.5.7, the amount of mixed rangeland that were converted into forest, grassland, farmland, built-up areas and bare soil only accounted for only 1638 hectares which barely equals half the amount of mixed rangeland that were converted into grassland in the previous observation data.

2005	2011 (Area in ha)						
	Forest	Mixed rangeland	Grassland	Farmland	Built-up	Bare soil	Water
Forest	140277.96	4025.97	79.47	685.62	127.71	196.2	157.41
Mixed Rangeland	431.37	261185.9	181.98	481.41	433.35	405.63	115.92
Grassland	0	2.07	38356.83	0.27	0.18	7.02	0.09
Farmland	0	0	0	24755.58	26.37	1.98	10.89
Built-up	0	0	0	0	4949.82	0	0
Soil	0	2.97	0.09	5.04	0.09	18452.88	0.54
Water	0	0	0	0	0	0	6126.84

Table 5.6.5. Matrix of land cover change from 2005 to 2011

Overall, between 1972 and 2011 there was a 17% of reduction in forest cover. This is 1% higher than the value reported by Erikstad et al (2001) in their previous bi-temporal LULC study for the entire country between 1972 and 1999 (Bouma and Kobryn, 2001). This small increase could be the result of gain and loss of forest after the past four decades. As shown in Figure 5.6.1, a significant amount of forest cover was cleared and only small amount of areas were gained between 1972 and 2011. The loss of forest were mainly the conversion from forest to mixed rangeland, grassland, farmland and built-up areas while gain in the amount of

forest mostly come from the conversion of mixed rangeland and grassland. Figure 5.6.2 shows “from-to” change that occurred between 1972 and 2011. Note that for visualization purpose only major categorical changes are shown in this map (i.e., forest, mixed rangeland and grassland).

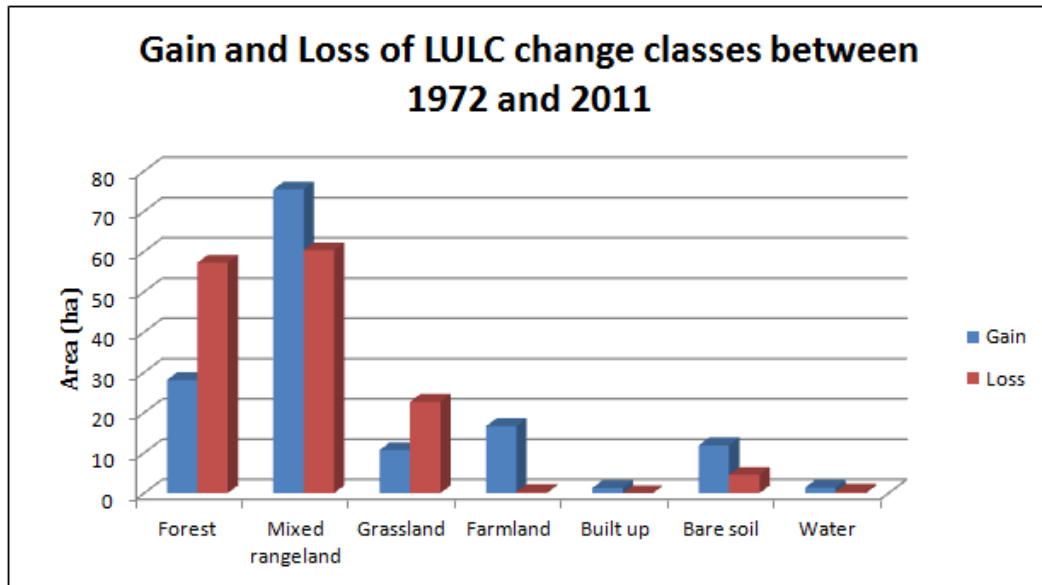


Figure 5.6.1. Gain and loss of LULC change classes between 1972 and 2011

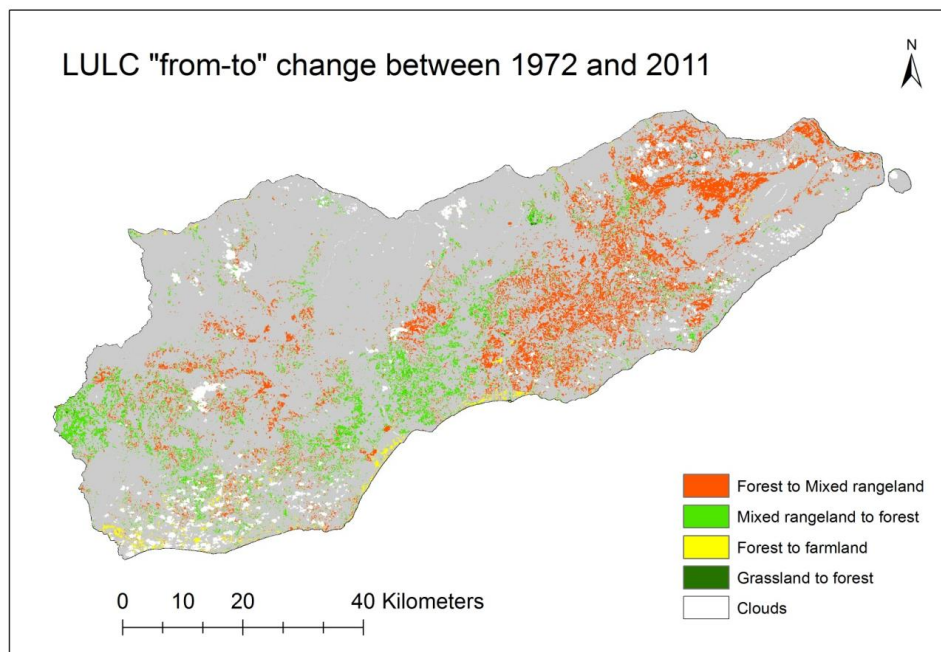


Figure 5.6.2. “From-to” major categorical change map between 1972 and 2011

The results from change detection indicated that the reduction of forest occurred primarily in the district of Lautem toward the eastern part of the study area (Figure 5.6.2 and Figure 5.6.3). In contrast, gain in the amount of forest area occurred mostly in Baucau and Viqueque districts (Figure 5.6.4). This trend could be explained through three main reasons.

First, the uncontrollable practice of logging during Indonesian occupation of East Timor during which timbers were cut not only for domestic use but also for the black market. Previous studies have also considered the argument that during Indonesia's occupation of East Timor, the military promoted logging as a means to suppress the resistance movement of East Timor's guerrillas (Aditjondro, 1994). This resulted in deforestation even in area where agricultural expansion did not exist, such as Lautem.

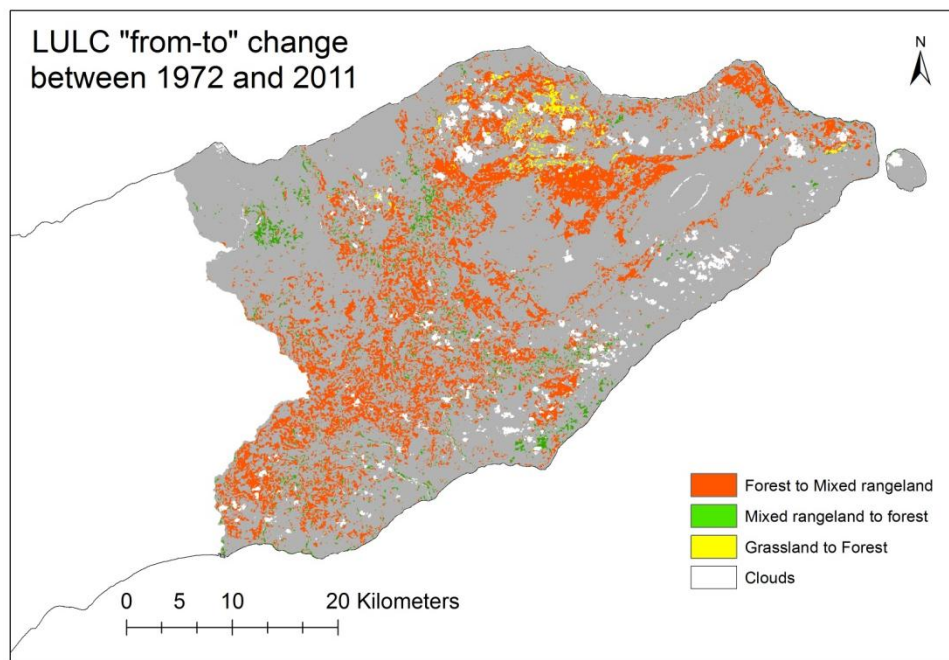


Figure 5.6.3. "From-to" change between 1972 and 2011 in Lautem district

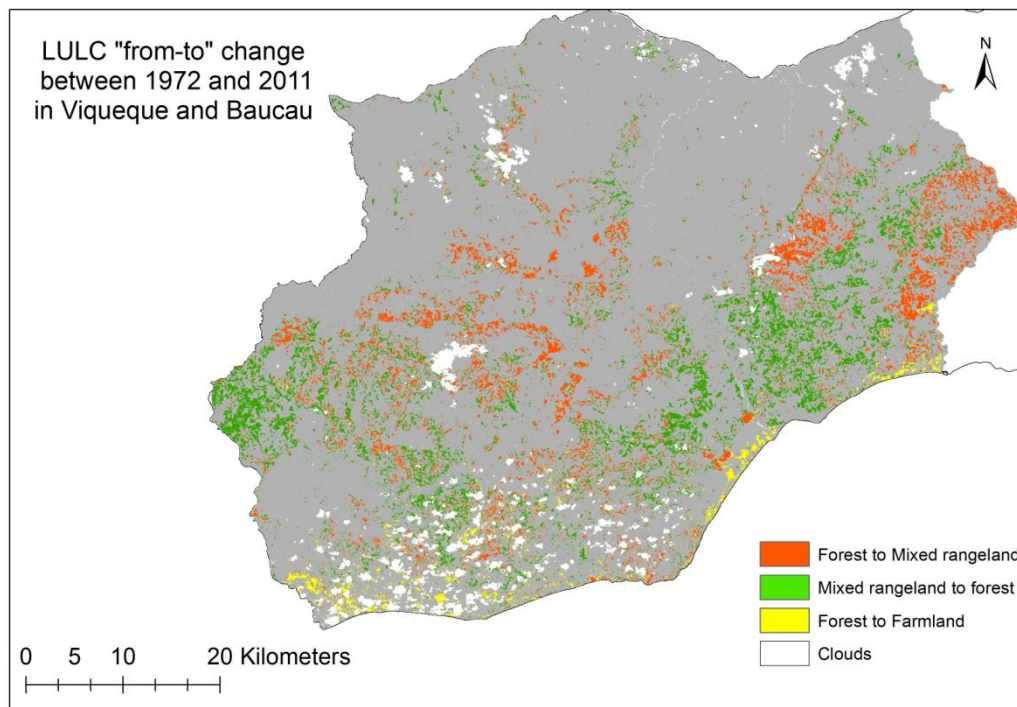


Figure 5.6.4. "From-to" change between 1972 and 2011 in Baucau and Viqueque districts

Second, during Indonesian occupation of East Timor, the government implemented a demographic policy by which villagers were encouraged to relocate to other remote areas. As a consequence, more lands were cleared and deforested to make way for new villages, settlements and farmlands. In the study area, especially in Viqueque, the effect of this transmigration policy is still apparent today with well regulated settlements and existence of shifting cultivation practices (Sundland et al., 2001)

Third, while most rice production occur in the lowland area, a substantial proportion of the farmland/plantation in the study area is areas with greater incline, where slope stability and erosion tend to be major problems. A recent study by Adams (2010) stated that nearly half the total area of East Timor is on steep slope (above 25 degrees). In these areas of steep slope, community villagers often practice slash-and-burn, swidden agriculture. Thus, these steep farmlands tend to suffer from rapid soil erosion and nutrient depletion, which forces farmers to find

new land and forest to meet their growing needs, so farmers could have moved towards the forested area for their agricultural activities.

5.7. Influence of 2000 map

A number of uncertainty-related issues in this study need to be addressed and recognized. First and foremost is the unavailability of map accuracy assessment for all maps other than 2000 map. These maps were generated by combining change maps, identified through NDVI differencing, with maps generated from unsupervised classification. Since the 2000 map was used as starting point (reference map) for final classification of all the other maps, a large portion of pixels from 2000 map is present in all the other maps. In other words, if an assumption was made that changes had not occurred over the past 40 years, the distribution of land use/cover in the study area would be similar to that depicted by the 2000 map. Under no change scenario, errors in each map would be correlated. However, in the change trajectory test, only 55% of the no change pixels were captured from the combined maps, which may also mean that only half of the total pixels of each map that has correlation (in terms of accuracy) with the map of 2000. In addition, the selection of threshold values for change/no change maps were merely conducted by visual inspection which also makes it difficult to estimate the accuracy.

5.8. Change rationality rules

The focus of this study is to detect land use/cover change with emphasis on forest cover change. Thus, the rules applied in the change trajectory evaluation test were based on the characteristic of land use/cover change in East Timor. These characteristics, or change behavior, were defined solely based on information and studies that linked expansion of agricultural lands, population growth, and increased shifting cultivation practices to deforestation. Clearly, this is somewhat an oversimplification of the true drivers of deforestation, which are far more complex than rules defined in this study (Lambin et al., 2001). Limitations of these

rules are recognized by the fact that increase in farmland occurred primarily in the southern coast (Viqueque district) but less in Lautem, even though large proportion of deforestation occurred in Lautem. In addition to that, while the rule was established based on the notion that deforestation occur due to urban growth and agricultural expansion, the change detection in this study revealed that large amount of forest were converted into mixed rangeland and not farmland. However, suffice to say that application of these rules can capture large part of land use/cover change behavior in the study area.

5.9. Potential of Approach

So far, with the exception of bio-temporal studies by Bouma and Kobryn (2004) and Erikstad et al (2001), there has not been a multi-temporal LULC change studies in East Timor. Therefore it is difficult to conduct a meaningful comparison between the result from this study and other studies. However, the potential of this approach could be improved with adequate field data in order to define better information and spectral classes. Furthermore, higher-ground-resolution satellite imagery could be used to detect LULC changes in this small-structured study area.

CHAPTER 6

6.1. CONCLUSION

This study has attempted to detect land use/cover change in the eastern part of East Timor between 1972 and 2011 using Landsat images with limited ground truth information. Using calibration information that came with satellite data, all the images were radiometrically and atmospherically corrected using widely used technique such as Dark-Object Subtraction (DOS).

A combination of supervised and unsupervised classification techniques were employed to derive maps for all the observation dates. These maps were combined with change/no change maps generated through NDVI differencing method to derive final classification maps for each observation dates. Furthermore, a simple rule-based rationality test was performed to evaluate changes between pixels in the final classification maps. A total of 5572060 number pixels were tested and the result shows that 3072292 number of pixels were identified as no change throughout the six observation dates (55%) and were labeled as 'correct'. 'Uncertain' pixels were then reclassified using information from 2000 map.

By applying post-classification comparison change detection technique the study reveals that between 1972 and 2011, 17% of forested land was cleared from the area although some gain from other LULC classes was also identified. By comparing it with study from Erikstad et al (201) it was concluded the amount of forest cover loss in the eastern half of East Timor was 1% higher than the total amount of loss reported by Erikstad et al (2001) for the entire country.

6.2. Limitations

Several constrains were encountered in this multi-temporal study of land cover change and attempts were made to minimize them. These constrains include lack of historical spatial data on land use/cover maps, reference data, and combination of

input data with varying spatial and spectral resolutions (MSS, TM, and ETM+). Data from MSS sensor (1972 images) had 79m x 79m spatial resolution with 4 bands compared to TM and ETM+ images which had 30m x 30m resolution and higher spectral resolution. Resampling of MSS data to match TM were necessary to make them comparable.

Another constrain was the limited availability of cloud-free images for the much preferred dates which made it difficult to obtain the images of anniversary dates. Originally, the study was planned to look at land cover change between 1972 and 2012. However, due to large contamination of clouds in the 2012, the 2011 image of ETM+ was selected instead. The choice of time interval between observation dates was also based on the availability of cloud free images.

The biggest limitation was the lack of reference data for all the observation dates. Much of spatial data that were produced prior to 2000 were supposedly kept by Indonesian mapping agency. A correspondence with this agency revealed that these spatial data no longer exist in their possession. Additionally, reports and publication about East Timor's past socio-demographic and land use characteristic were only held by foreign library in hard-copy format. Therefore, simple methodology for evaluating the land cover change was a necessary mean. And although this study shows a satisfying result, it is critical to note that there is some degree, if not great, of misclassification and class confusion in the change detection analysis due to the aforementioned limitations.

Therefore, based on the limitations and findings from this study, it is recommended that future studies be conducted in such a way that incorporates more reliable data with better spatial, spectral and temporal resolution. It's also recommended that mapping entities in East Timor strengthen their efforts to make necessary spatial data available not only for internal use but also for the public at large. This could be accomplished through an increased collaborative work with foreign institutions

(both governmental and non-governmental) that hold spatial data (digital and archival) in their possession.

BIBLIOGRAPHICAL REFERENCES

- Adams, D. (2010). Land Use Survey and Land Use Database and Information System Development in Timor-Leste. *UNDP – SLM Project*.
- Anderson, J. , Hardy, E. E., Roach, J. T., Witmer, R. E. (1976). *A land use and land cover classification system for use with remote sensor data* (Vol. 964). A revision of the land use classification system as presented in U.S. Geological Survey Circular 671. US Government Printing Office.
- Anderson, M. C., Allen, R. G., Morse, A., & Kustas, W. P. (2012). Use of Landsat thermal imagery in monitoring evapotranspiration and managing water resources. *Remote Sensing of Environment*
- Baraldi, A., Bruzzone, L., & Blonda, P. (2005). Quality assessment of classification and cluster maps without ground truth knowledge. *Geoscience and Remote Sensing, IEEE Transactions on*, 43(4), 857-873
- Bouma, G. A., & Kobryn, H. T. (2004, February). Change in vegetation cover in East Timor, 1989–1999. In *Natural resources forum* (Vol. 28, No. 1, pp. 1-12). Blackwell Publishing Ltd.
- Campbell, J. B., & Wynne, R. H. (2011). *Introduction to Remote Sensing. (No. ed. 5)*. Guildford Press.
- Canada Center for Remote Sensing (CCRS) (n.d.). Fundamentals of of Remote Sensing. Available at http://www.nrcan.gc.ca/sites/www.nrcan.gc.ca/earth-sciences/files/pdf/resource/tutor/fundam/pdf/fundamentals_e.pdf
- Chander, G., Markham, B. L., & Helder, D. L. (2009). Summary of current radiometric calibration coefficients for Landsat MSS, TM, ETM+, and EO-1 ALI sensors. *Remote sensing of environment*, 113(5), 893-903
- Chavez, P. S. (1988). An improved dark-object subtraction technique for atmospheric scattering correction of multispectral data. *Remote Sensing of Environment*, 24(3), 459-479.
- Chavez, P. S. (1996). Image-based atmospheric corrections-revisited and improved. *Photogrammetric engineering and remote sensing*, 62(9), 1025-1035.
- Congalton, R. G., & Green, K. (2008). *Assessing the accuracy of remotely sensed data: principles and practices*. CRC.
- Costa Carvalho, C. A. (1972). Coordenadas da população de Timor-Leste. Instituto Nacional da Estatística.
- Da Costa, H. (2003). *Agriculture--new directions for a new nation: East Timor (Timor-Leste): proceedings of a workshop 1-3 October 2002, Dili, East Timor* (No. 113). Australian Centre for International Agricultural Research.
- Doraiswamy, P. C., Moulin, S., Cook, P. W., & Stern, A. (2003). Crop yield assessment from remote sensing. *Photogrammetric engineering and remote sensing*, 69(6), 665-674.

Erikstad, L., Bakkestuen, V., Sandlund, O.T., (2001). Deforestation in East Timor since 1972 as indicated by LANDSAT imagery. Annex 6. In: Sandlund, O.T., Bryceson, I., de Carvalho, D., Rio, N., da Silva, J., Silva, M.I. (Eds.), *Assessing Environmental Needs and Priorities in East Timor. Final Report*. NINA-NIKU, Foundation for Nature Research and Cultural Heritage Research, Trondheim, Norway.

Foody, G. M. (2010). Assessing the accuracy of land cover change with imperfect ground reference data. *Remote Sensing of Environment*, 114(10), 2271-2285.

ESRI (2010). How Iso Cluster Works. Available at http://help.arcgis.com/en/arcgisdesktop/10.0/help/index.html#/How_Iso_Cluster_works/009z000000q8000000/

FAO (2010). Global Forest Resources Assessment. *Main Report*. FAO Forestry Paper, 163

Ghoneim, E. (2009). A remote sensing study of some impacts of global warming on the Arab region. *Impacts of climate changes on the Arab countries*. Chapter 3, 31 – 46

Goldewijk, K. K., & Ramankutty, N. (2004). Land use change during the past 300 years. *Land Use Land Cover and Soil Sciences – Vol. I – Encyclopedia of Life Support System (EOLSS)*

Hayes, D. J., & Sader, S. A. (2001). Comparison of change-detection techniques for monitoring tropical forest clearing and vegetation regrowth in a time series. *Photogrammetric engineering and remote sensing*, 67(9), 1067-1075.

Ioannis, M., & Meliadis, M. (2011). Multi-temporal Landsat image classification and change analysis of land cover/use in the Prefecture of Thessaloiniki, Greece. *Proceedings of the International Academy of Ecology and Environmental Sciences*, 1(1), 15-25.

Jensen, J. R. (2005). *Introductory digital image processing: a remote sensing perspective* (No. Ed. 2). Prentice-Hall Inc

Jensen, J. R. (2007). *Remote Sensing of the Environment: An Earth Resource Perspective*, (No. Ed. 2). Upper Saddle River, NJ: Prentice Hall.

Jeus, M., Henriques, P., Laranjeir, P., Narciso, V., Carvalho, M. L. da S., (2012). The impact of shifting cultivation in the forestry ecosystem of Timor-Leste. *Centro de estudos e formação avançada em gestão e economia*.

Lambin, E. F., Geist, H. J., & Lepers, E. (2003). Dynamics of land-use and land-cover change in tropical regions. *Annual review of environment and resources*, 28(1), 205-241.

Lambin, E. F., Turner, B. L., Geist, H. J., Agbola, S. B., Angelsen, A., Bruce, J. W., ... & Xu, J. (2001). The causes of land-use and land-cover change: moving beyond the myths. *Global environmental change*, 11(4), 261-269.

Lillesand, T. M., Kiefer, R. W., & Chipman, J. W. (2004). *Remote sensing and image interpretation* (No. Ed. 5). John Wiley & Sons Ltd.

- Liu, H., & Zhou, Q. (2004). Accuracy analysis of remote sensing change detection by rule-based rationality evaluation with post-classification comparison. *International Journal of Remote Sensing*, 25(5), 1037-1050.
- Lu, D., Mausel, P., Brondízio, E., & Moran, E. (2004). Change detection techniques. *International Journal of Remote Sensing*, 25(12), 2365-2401.
- Macleod, R. D., & Congalton, R. G. (1998). A quantitative comparison of change-detection algorithms for monitoring eelgrass from remotely sensed data. *Photogrammetric Engineering and Remote Sensing*, 64(3), 207-216.
- Martinuzzi, S., Gould, W. A., & González, O. M. R. (2007). *Creating cloud-free Landsat ETM+ data sets in tropical landscapes: cloud and cloud-shadow removal*. US Department of Agriculture, Pacific Northwest Research Station.
- Masek, J. G., Lindsay, F. E., & Goward, S. N. (2000). Dynamics of urban growth in the Washington DC metropolitan area, 1973-1996, from Landsat observations. *International Journal of Remote Sensing*, 21(18), 3473-3486.
- Mau, Raimundo (n.d.). In *Methodology of Research*.
- Mertens, B., & Lambin, E. F. (2000). Land-cover-change trajectories in southern Cameroon. *Annals of the association of American Geographers*, 90(3), 467-494.
- MAF (2001). Rapid Rural Land Use Assessment and Model for Land Use Classification and Mapping. Agricultural land use and GIS unit.
- NSD (2011). Population and Housing Census of Timor-Leste, 2010
- PANCROMA (2012). Gap filling using Hayes method.
- Pederson, J. and M. Arneberg (1999). Social and Economic Conditions in East Timor, New York: Columbia University International Conflict Resolution Program, School of International and Public Affairs/Oslo: Fafo Institute of Applied Social Science
- Petit, C., Scudder, T., & Lambin, E. (2001). Quantifying processes of land-cover change by remote sensing: resettlement and rapid land-cover changes in south-eastern Zambia. *International Journal of Remote Sensing*, 22(17), 3435-3456.
- Pontius Jr, R. G., & Millones, M. (2011). Death to Kappa: birth of quantity disagreement and allocation disagreement for accuracy assessment. *International Journal of Remote Sensing*, 32(15), 4407-4429.
- Pu, R., Gong, P., Tian, Y., Miao, X., Carruthers, R. I., & Anderson, G. L. (2008). Using classification and NDVI differencing methods for monitoring sparse vegetation coverage: a case study of saltcedar in Nevada, USA. *International Journal of Remote Sensing*, 29(14), 3987-4011.
- Rahman, M. R., Islam, A. H., & Hassan, M. S. (2004). Change Detection of Winter Crop Coverage and the use of LANDSAT Data with GIS.

Sandlund, O. T., Bryceson, I., de Carvalho, D., Rio, N., da Silva, J., & Silva, M. I. (2001). Assessing environmental needs and priorities in East Timor: issues and priorities. *UNDP and Norwegian Institute for Nature Research, Norway*.

Scaramuzza, P., Micijevic, E., & Chander, G. (2004). SLC gap-filled products: Phase one methodology. *Landsat Technical Notes*

Singh, A. (1989). Review Article Digital change detection techniques using remotely-sensed data. *International journal of remote sensing*, 10(6), 989-1003.

Sobrino, J. A., Jiménez-Muñoz, J. C., & Paolini, L. (2004). Land surface temperature retrieval from LANDSAT TM 5. *Remote Sensing of Environment*, 90(4), 434-440.

Symeonakis, E., & Drake, N. (2004). Monitoring desertification and land degradation over sub-Saharan Africa. *International Journal of Remote Sensing*, 25(3), 573-592.

Zhang, C., Li, W., & Travis, D. (2007). Gaps-fill of SLC-off Landsat ETM+ satellite image using a geostatistical approach. *International Journal of Remote Sensing*, 28(22), 5103-5122.

Yuan, F., Sawaya, K. E., Loeffelholz, B. C., & Bauer, M. E. (2005). Land cover classification and change analysis of the Twin Cities (Minnesota) Metropolitan Area by multitemporal Landsat remote sensing. *Remote sensing of Environment*, 98(2), 317-328.

APPENDIX A

Change/no change pixels generated from NDVI differencing technique

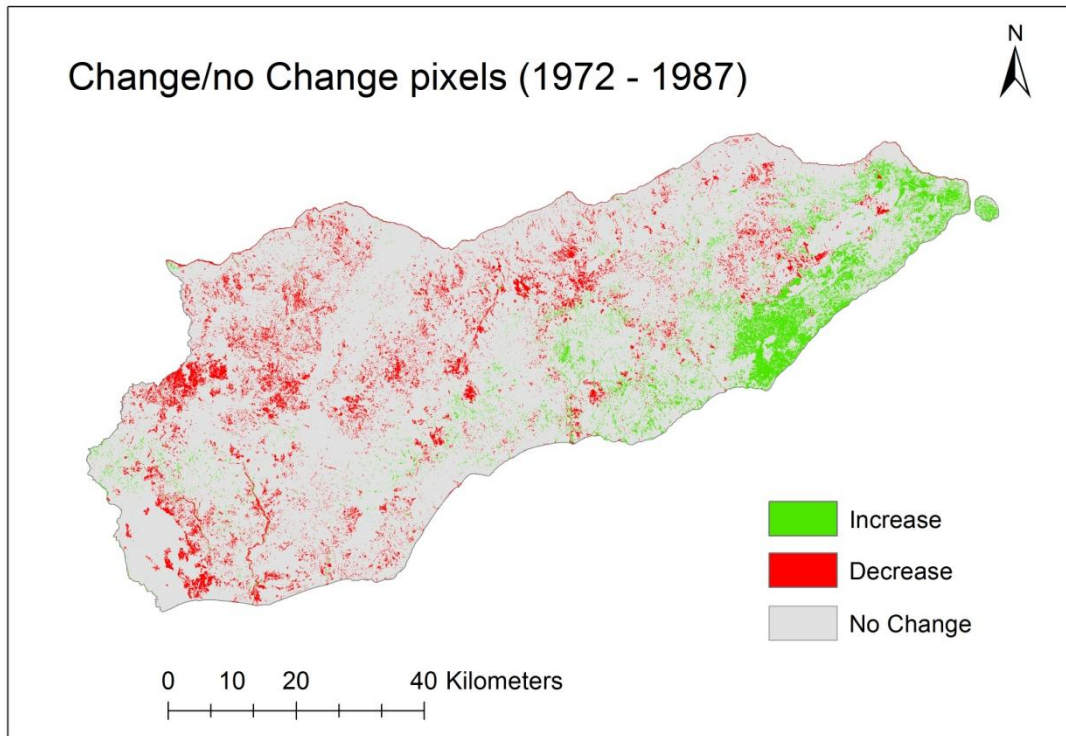


Figure A.1. Change/no change pixels for the year 1972 and 1987

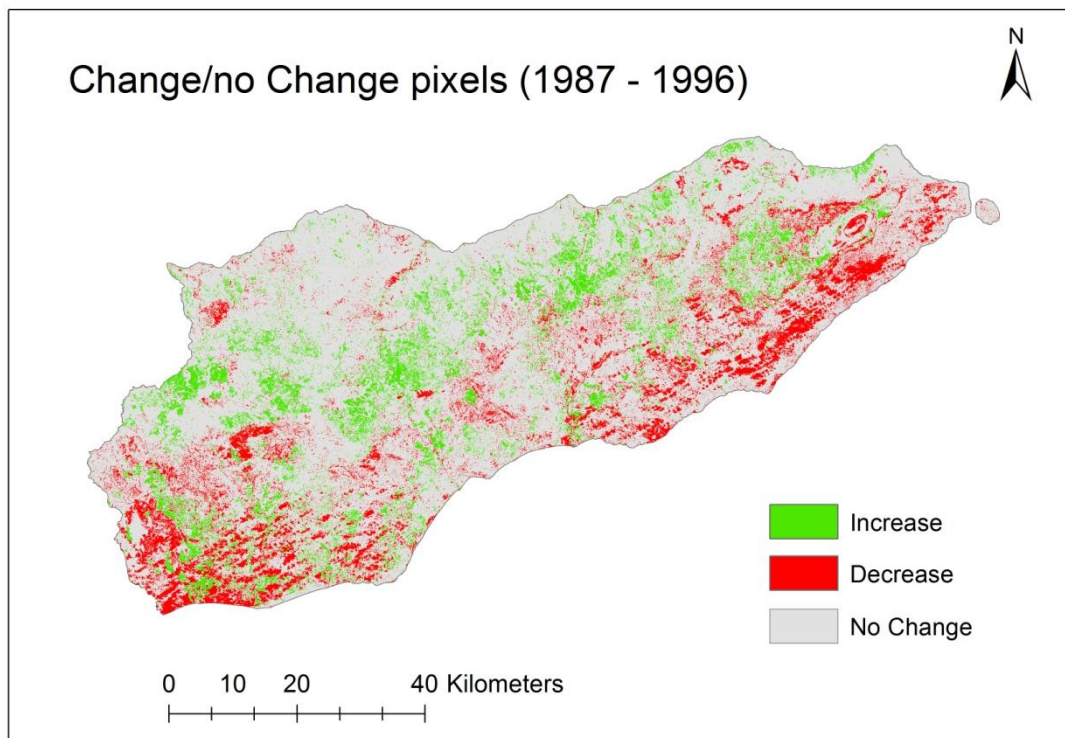


Figure A.2. Change/no change pixels for the year 1987 and 1996

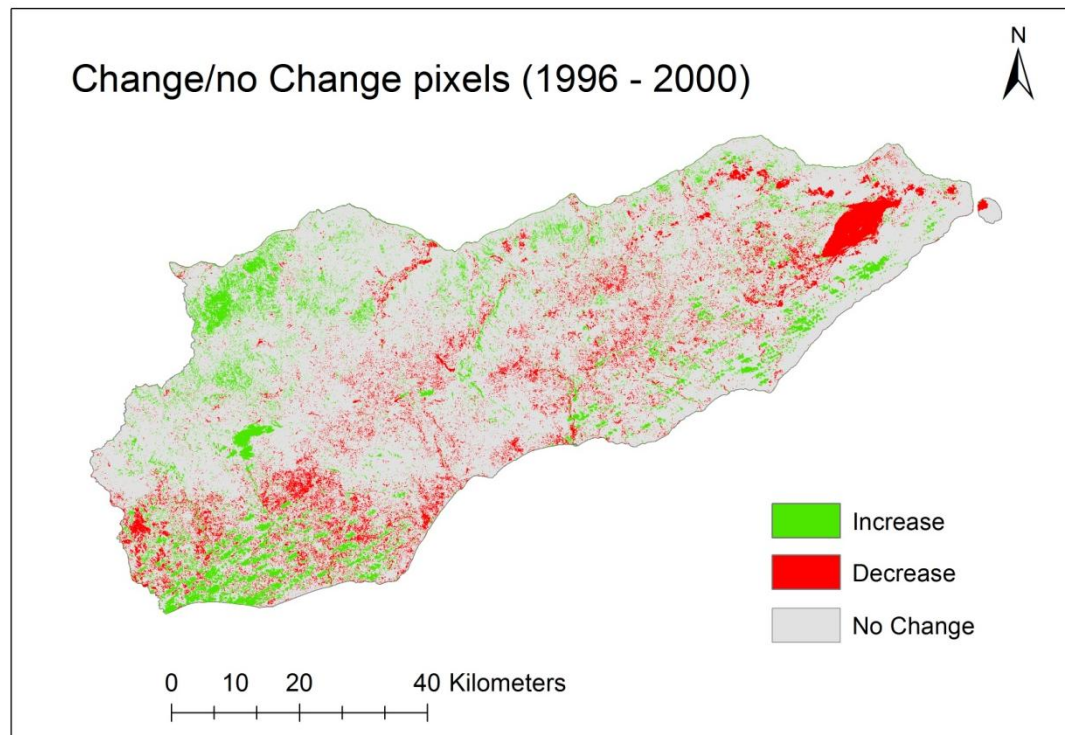


Figure A.3. Change/no change pixels for the year 1996 and 2000

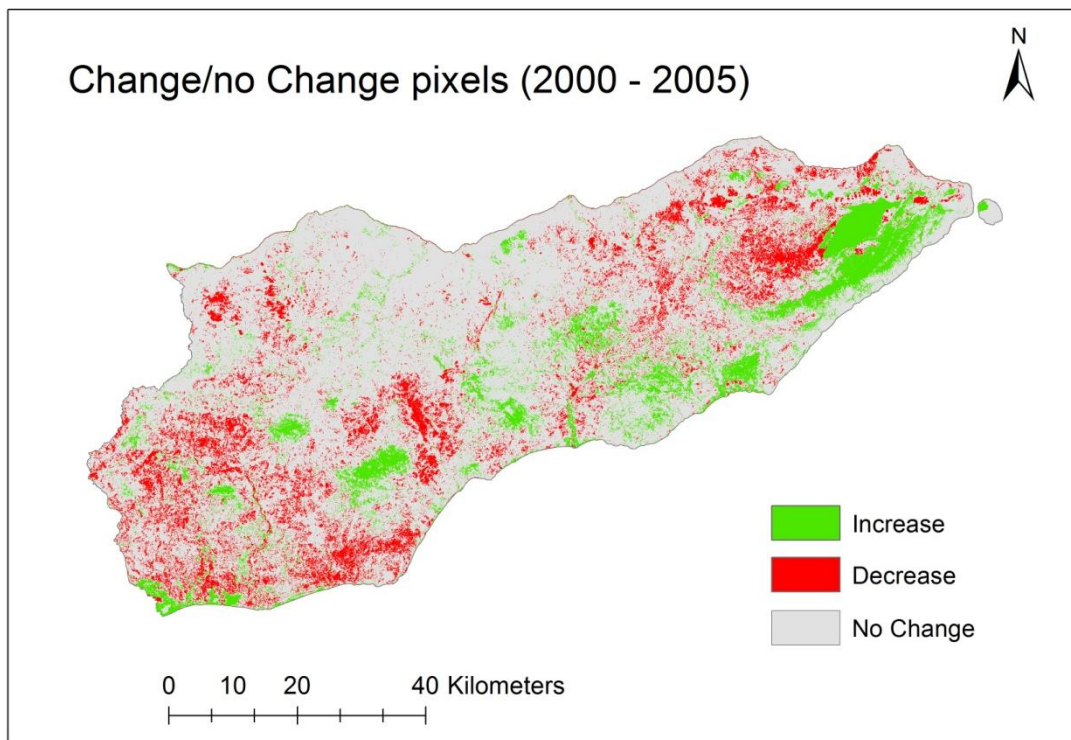


Figure A.3. Change/no change pixels for the year 2000 and 2005

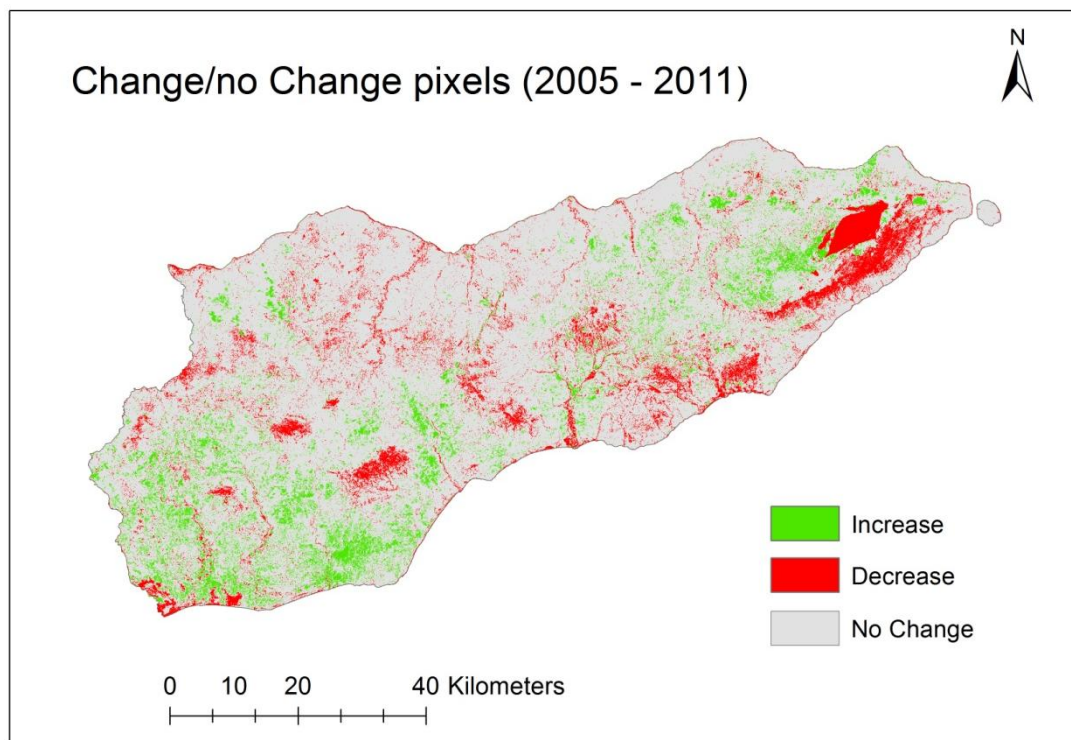


Figure A.3. Change/no change pixels for the year 2005 and 2011

APPENDIX B

Final Classification maps generated by combining change maps (NDVI differencing) and classified maps (supervised and unsupervised)

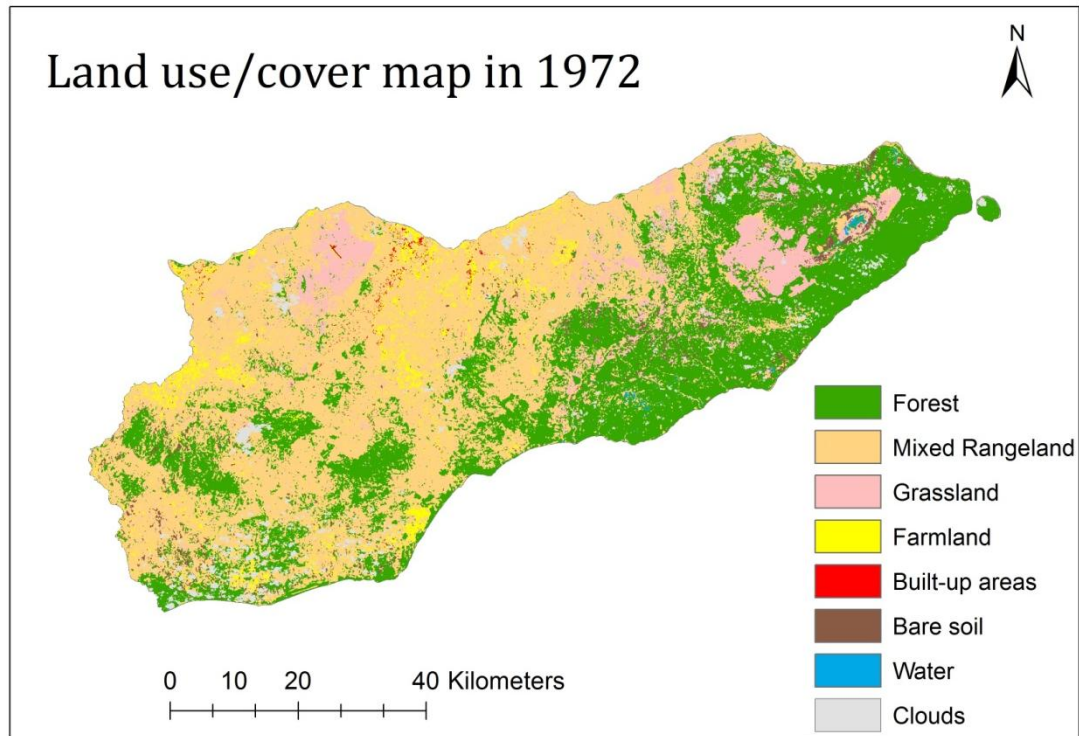


Figure B.1. Final LULC map for the year 1972

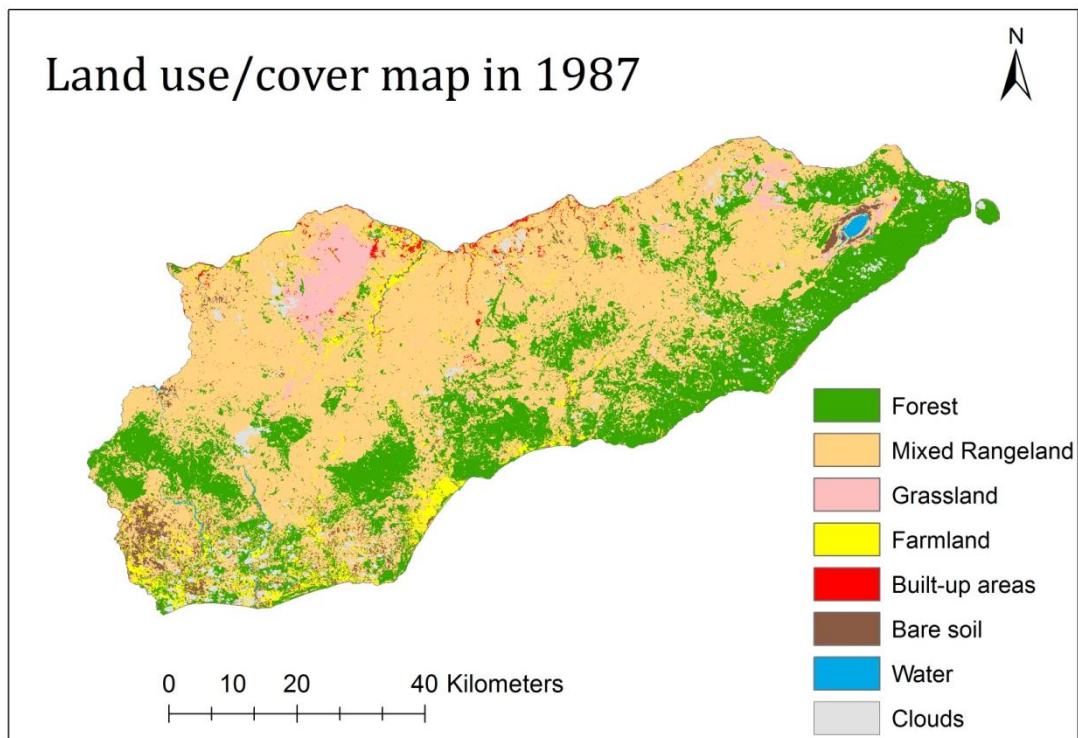


Figure B.2. Final LULC map for the year 1987

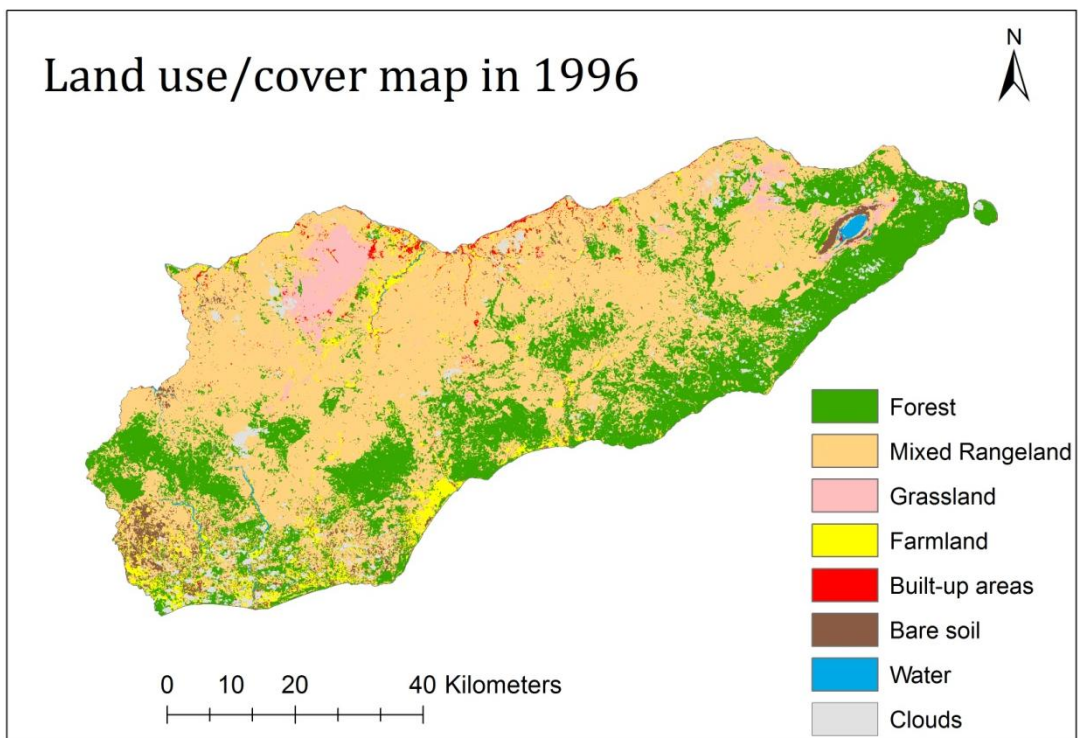


Figure B.3. Final LUL map for the year 1996

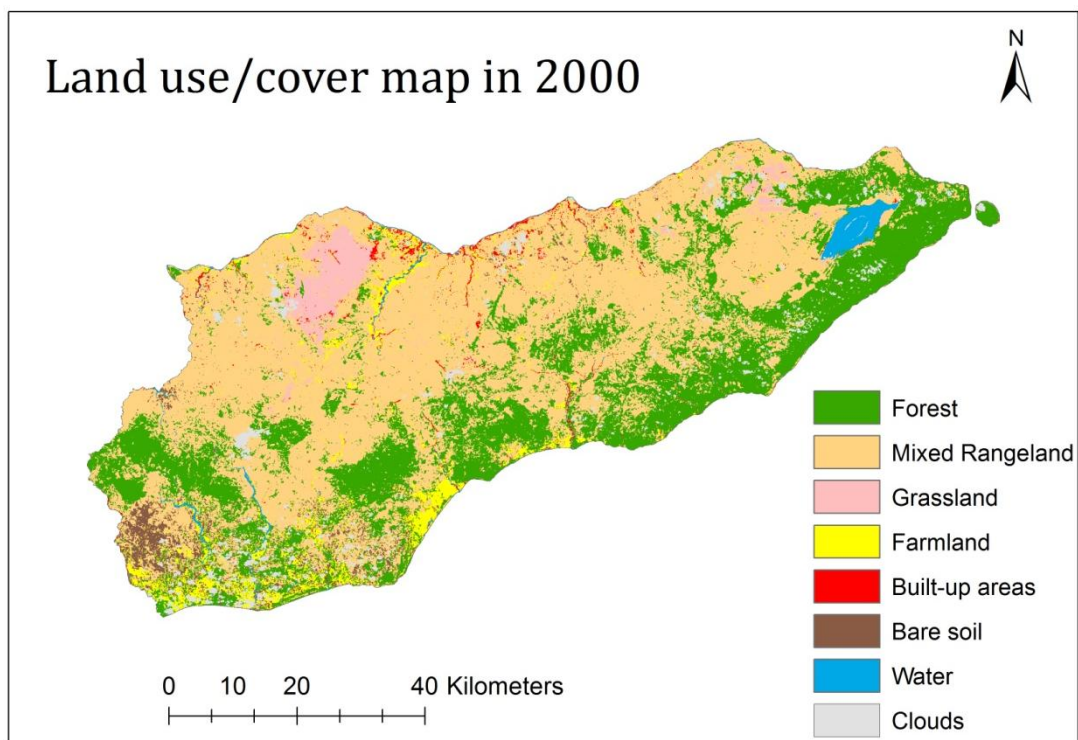


Figure B.4. Final LULC map for the year 2000

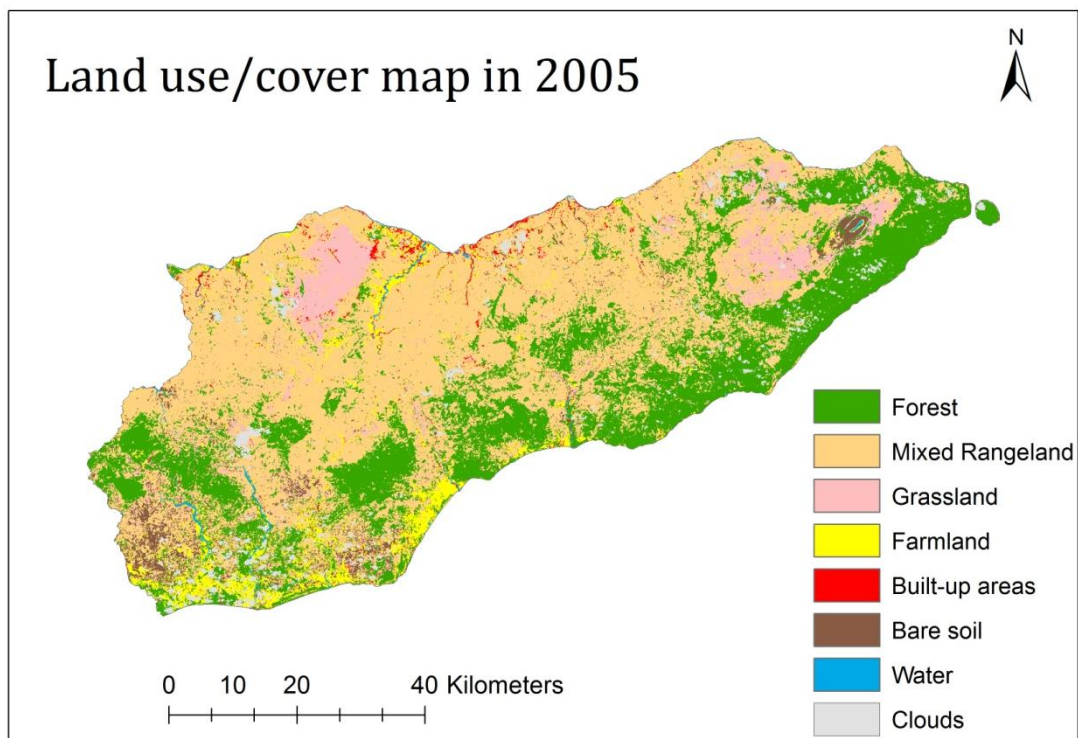


Figure B.5. Final LULC map for the year 2005

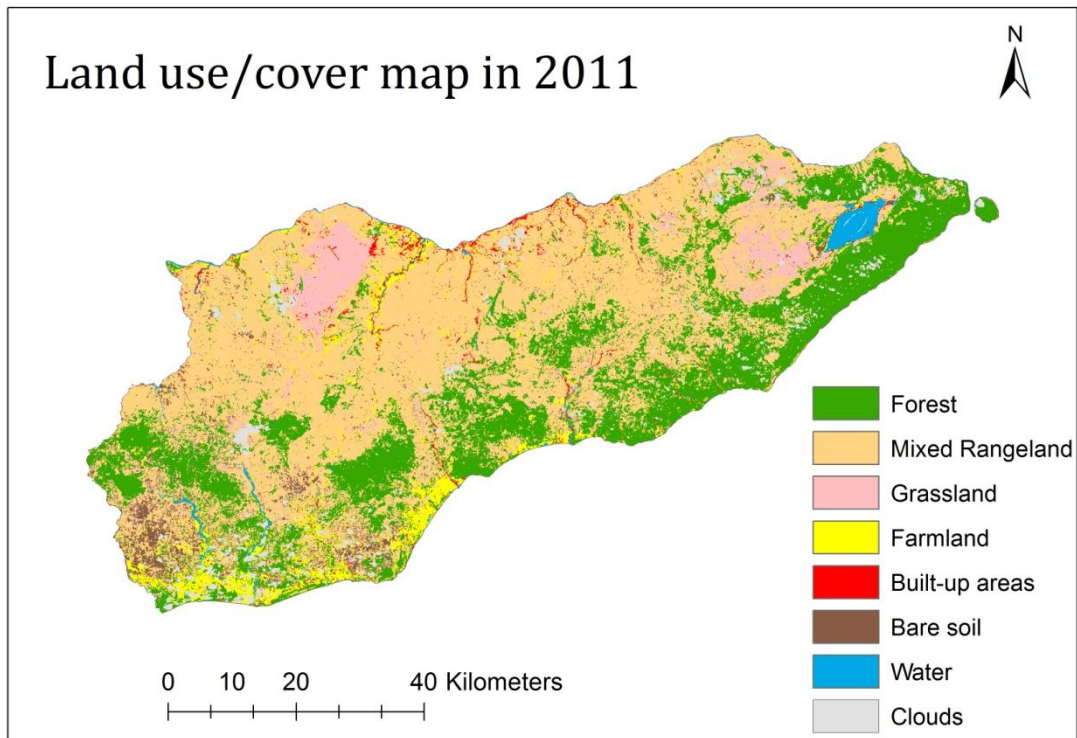


Figure B.6. Final LULC map for the year 2011

APPENDIX C

Sensor	Date of Acquisition	Bands	Lmax	Lmin	d	E_{sun}	Sun elevation
MSS	Oct 4, 1972	Band 1	201.000	0.000	1.00005	1823	33.04947919
		Band 2	171.300	9.100	1.00005	1559	33.04947919
		Band 3	161.600	-8.400	1.00005	1276	33.04947919
		Band 4	159.000	0.000	1.00005	880.1	33.04947919
MSS	Oct 23, 1972	Band 1	201.000	0.000	0.99467	1823	31.43913809
		Band 2	171.300	9.100	0.99467	1559	31.43913809
		Band 3	161.600	-8.400	0.99467	1276	31.43913809
		Band 4	159.000	0.000	0.99467	880.1	31.43913809
TM	Sept 8, 1987	Band 1	169.000	-1.520	1.00750	1983	38.7524847
		Band 2	333.000	-2.840	1.00750	1796	38.7524847
		Band 3	264.000	-1.170	1.00750	1536	38.7524847
		Band 4	221.000	-1.510	1.00750	1031	38.7524847
		Band 5	30.200	-0.370	1.00750	220.0	38.7524847
		Band 7	16.500	-0.150	1.00750	83.4	38.7524847
TM	Aug 15, 1996	Band 1	169.000	-1.520	1.01281	1983	45.96315356
		Band 2	333.000	-2.840	1.01281	1796	45.96315356
		Band 3	264.000	-1.170	1.01281	1536	45.96315356
		Band 4	221.000	-1.510	1.01281	1031	45.96315356
		Band 5	30.200	-0.370	1.01281	220.0	45.96315356
		Band 7	16.500	-0.150	1.01281	83.4	45.96315356
ETM+	Sept 1, 2000	Band 1	191.600	-6.200	1.00850	1997	34.2739053
		Band 2	196.500	-6.400	1.00850	1812	34.2739053
		Band 3	152.900	-5.000	1.00850	1533	34.2739053
		Band 4	241.100	-5.100	1.00850	1039	34.2739053
		Band 5	31.060	-1.000	1.00850	230.8	34.2739053
		Band 7	10.800	0.350	1.00850	84.90	34.2739053
TM	Oct 11, 2005	Band 1	169.000	-1.520	0.99832	1983	27.7005789
		Band 2	365.000	-2.840	0.99832	1796	27.7005789
		Band 3	264.000	-1.170	0.99832	1536	27.7005789
		Band 4	221.000	-1.510	0.99832	1031	27.7005789
		Band 5	30.200	-0.370	0.99832	220.0	27.7005789
		Band 7	16.500	-0.150	0.99832	83.4	45.96315356
ETM+	Aug 17, 2011	Band 1	191.600	-6.200	1.01244	1983	37.8719668
		Band 2	196.500	-6.400	1.01244	1796	37.8719668
		Band 3	152.900	-5.000	1.01244	1536	37.8719668
		Band 4	241.100	-5.100	1.01244	1031	37.8719668
		Band 5	31.060	-1.000	1.01244	220.0	37.8719668
		Band 7	10.800	0.350	1.01244	83.4	37.8719668

Table C.2. Radiometric calibration coefficients for Landsat data used in this study

APPENDIX D

NDVI Maps for all observation dates

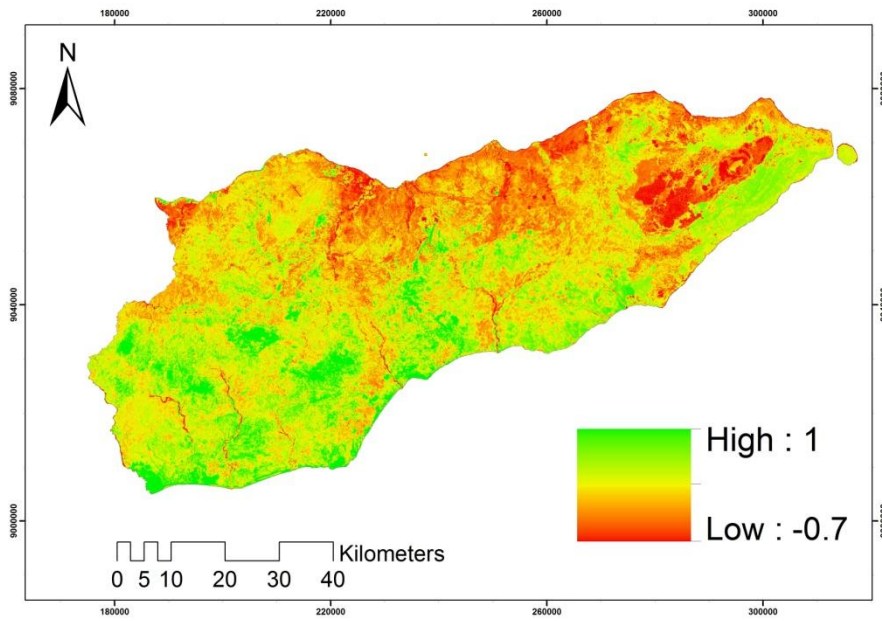


Figure D.1. NDVI of 1972

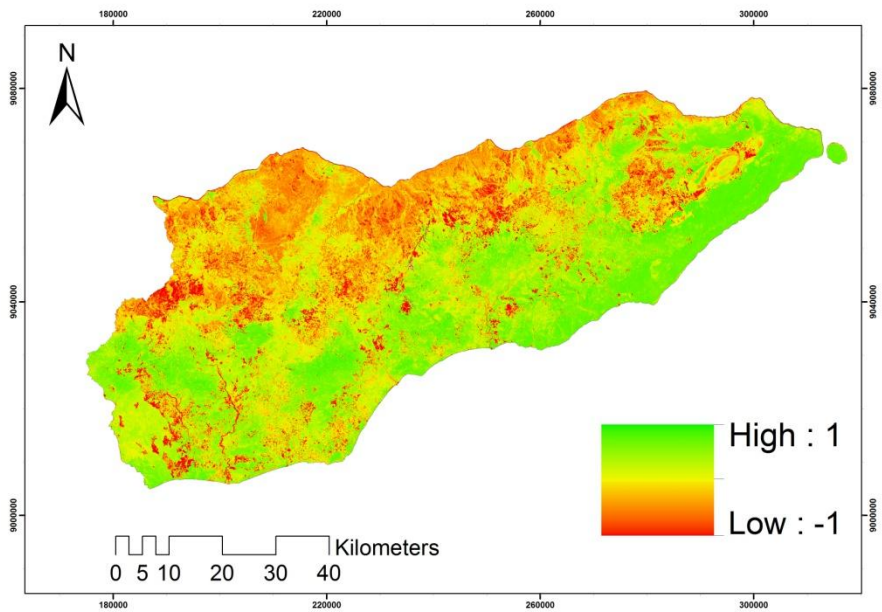


Figure D.2. NDVI of 1987

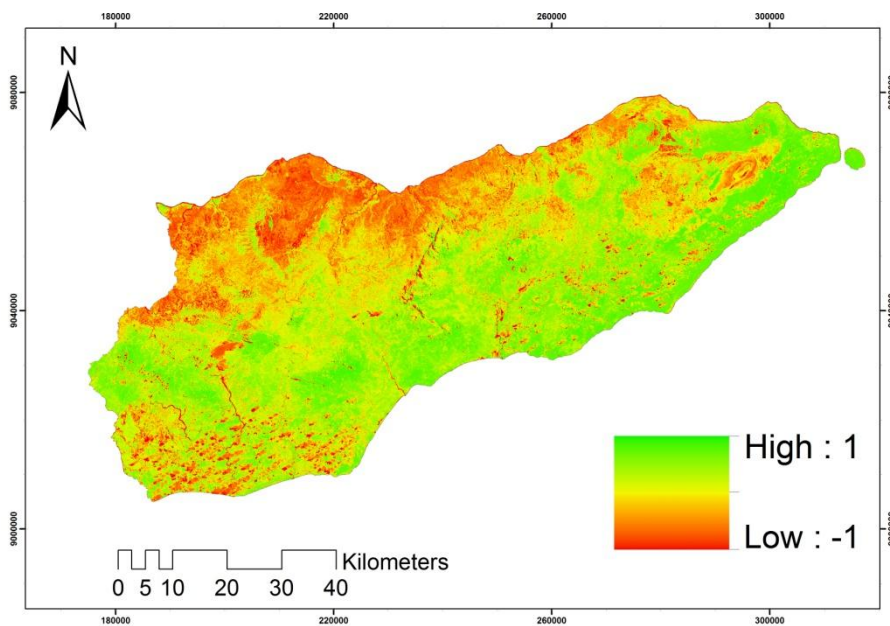


Figure D.3. NDVI of 1996

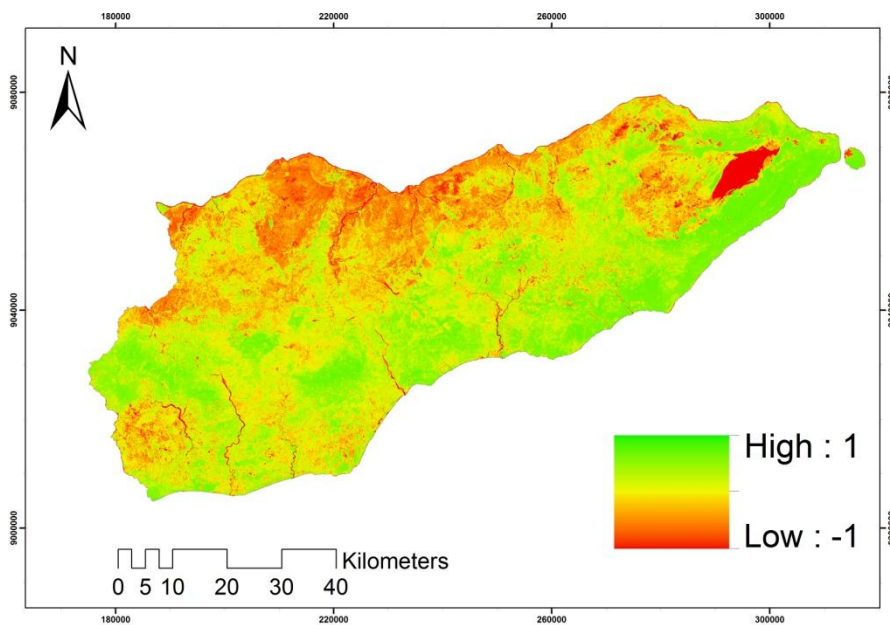


Figure D.4. NDVI of 2000

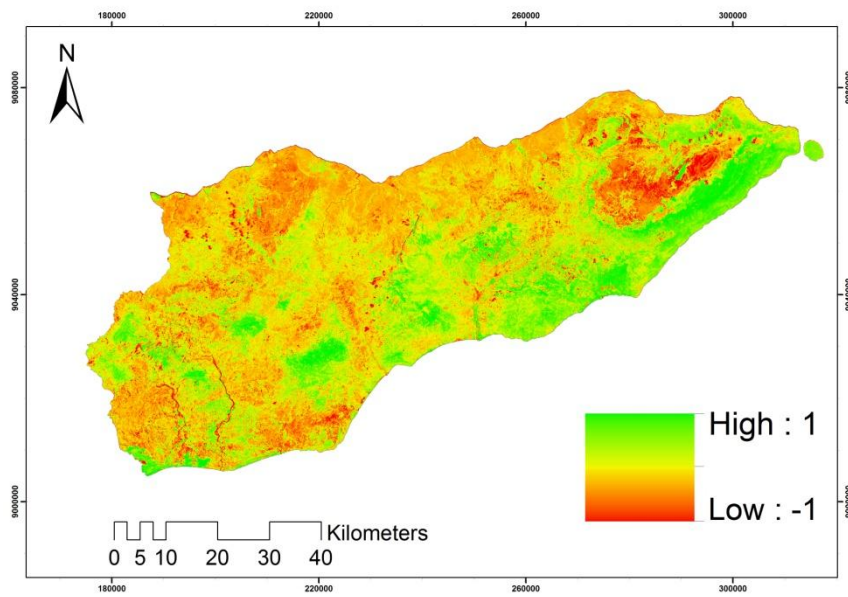


Figure D.5. NDVI of 2005

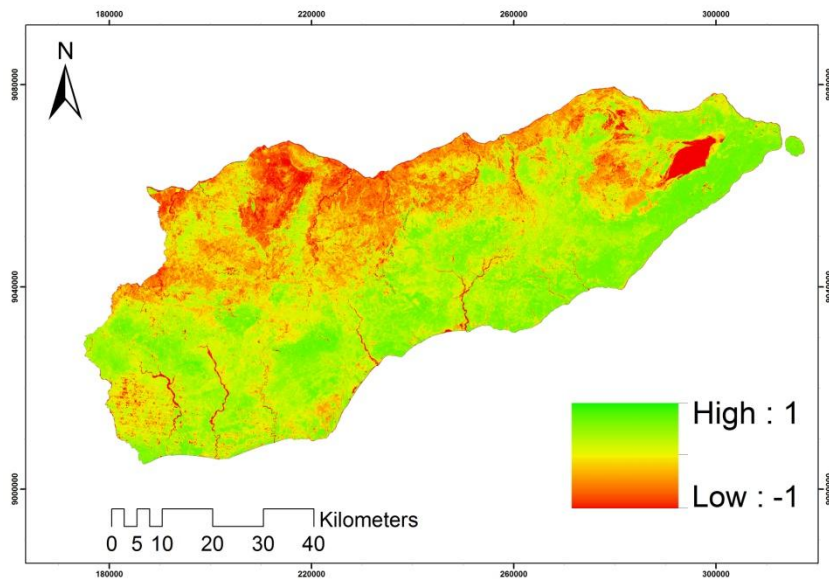


Figure D.6. NDVI 2011



Masters Program in **Geospatial Technologies**



Supported by:



Education and Culture
ERASMUS MUNDUS